Noname manuscript No.
(will be inserted by the editor)

On the origin of the faint-end of the red sequence in high density environments.

Alessandro Boselli · Giuseppe Gavazzi

arXiv:1411.5513v1 [astro-ph.GA] 20 Nov 2014

Received: 10/08/2014 / Accepted: 27/08/2014

Abstract With the advent of the next generation wide-field cameras it became possible to survey in an unbiased mode galaxies spanning a variety of local densities, from the core of rich clusters, to compact and loose groups, down to filaments and voids. The sensitivity reached by these instruments allowed to extend the observation to dwarf galaxies, the most "fragile" objects in the universe. At the same time models and simulations have been tailored to quantify the different effects of the environment on the evolution of galaxies. Simulations, models, and observations consistently indicate that star-forming dwarf galaxies entering high-density environments for the first time can be rapidly stripped from their interstellar medium. The lack of gas quenches the activity of star formation, producing on timescales of ∼1 Gyr quiescent galaxies with spectro-photometric, chemical, structural, and kinematical properties similar to those observed in dwarf early-type galaxies inhabiting rich clusters and loose groups. Simulations and observations consistently identify ram pressure stripping as the major effect responsible for the quenching of the star-formation activity in rich clusters. Gravitational interactions (galaxy harassment) can also be important in groups or in clusters whenever galaxies have been members since early epochs. The observation of clusters at different redshifts combined with the present high infalling rate of galaxies onto clusters indicate that the quenching of the star-formation activity in dwarf systems and the formation of the faint end of the red sequence is a very recent phenomenon.

Keywords Clusters · General · Evolution · Interactions · ISM · Star formation

Alessandro Boselli
Laboratoire d'Astrophysique de Marseille - LAM, Université d'Aix-Marseille & CNRS, UMR7326, 38 rue F. Joliot-Curie, F-13388 Marseille Cedex 13, France
Tel.: +33-491056976
Fax: +33-491621190
E-mail: alessandro.boselli@lam.fr

Giuseppe Gavazzi
Università di Milano - Bicoocca - Piazza della scienza 3, Milano - Italy
E-mail: gavazzi@mib.infn.it

1 Introduction

In 2006, the present authors reviewed the "Environmental effects on late-type galaxies (LTGs) in nearby clusters" (Boselli & Gavazzi 2006). Is there a compelling urgency for a new review on such a short time lag? The answer is yes, because the DR7 release of the Sloan Digital Sky Survey (SDSS, Abazajian et al. 2009) which disclosed the complete northern sky to photometric and spectroscopic observations to limits as faint as 17.7 (r) mag, was yet to come in 2006. Beside the SDSS, several panoramic multifrequency surveys of large stretches of the local Universe became available after 2006 (we will review them in Sect. 2). The crucial novelty of these surveys is that they allowed for the first time to sample clusters of galaxies *at large*, embedded in surrounding regions of relatively low galactic density, making it possible to contrast directly, not only by statistical means, the galaxy properties in ambients of significantly different density: cluster cores, cluster outskirts, loose groups, filaments, and voids.

Indeed, many other significant progresses in this field were achieved after 2006, concerning both the observations and the simulations which brought a deeper conviction that the environment—*nurture*—plays a relevant role on the evolution of galaxies, especially at the low-mass end. It is on the new evidences that the present review is focused. As in Boselli & Gavazzi (2006), Virgo, Coma, and A1367 and their surrounding superclusters, being among the best studied clusters, will dominate the discussion, and will be treated as representative of the local Universe.

The key motivation for environmental issues on galaxy evolution is that, no matter if galaxies spend most of their life in relatively low-density regions of space (the filaments of the cosmic web), a large fraction of them is sooner or later processed through denser (groups) and denser (clusters) environments. This picture clearly emerges from numerical simulations in the ΛCDM cosmology (e.g. the Millennium simulation, Springel et al. 2005), where satellite galaxies continuously feed regions of higher density (central galaxies, groups, clusters) at the intersection of multiple filaments. Even at $z = 0$ there is substantial evidence for high-velocity infall of "healthy" (star forming) galaxies into rich clusters, which also arises from the anisotropy of the velocity distribution of LTGs compared to early-type galaxies (ETGs) (see Fig. 14 of Boselli & Gavazzi 2006). Whereas ETGs obey to a Gaussian distribution, LTGs tend to populate the wings of the distribution at high and low velocity. Considering the time scales for the various transformations, Boselli et al. (2008a) and Gavazzi et al. (2013a,b) were able to estimate that infall on the Virgo (Coma) cluster occurred at a rate of approximately 300–400 (100) galaxies with mass $M_{\rm star} \gtrsim 10^9$ $M_\odot$ per Gyr in the last 2 (7.5) Gyrs.

We wish to begin and to close this review with Abell 1367, the prototypical laboratory for the study of galaxies under the influence of hydrodynamical processes. Figure 1 shows the distribution of its central galaxies from the SDSS. Also marked are two faint ($M_{\rm star} \sim 10^{9.5}$ $M_\odot$) CGCG galaxies 97073, 97079 next to 97087 that have projected distances less than one Mpc from the cluster X-ray center (well inside the virial radius of A1367 that was estimated 2.1 Mpc by Boselli & Gavazzi 2006). Gavazzi & Jaffe 1985 discovered their "head–tail" radio continuum emission (see color inset from Gavazzi et al. 1995) and Gavazzi et al. (2001) detected Hα emission trailing behind them for ~75 Mpc, an evident sign of high-velocity interaction with the ICM. The inset labeled "BIG" contains a compact group of blue galaxies infalling at 2,500 km s^{-1} into the main cluster (Sakai et al. 2002; Gavazzi et al. 2003b; Cortese et al. 2006a,b). Next to BIG, the elliptical galaxy NGC3862 (CGCG 97127), the brightest cluster member, harbors the head–tail radio galaxy 3C 264 (not shown in Fig. 1).

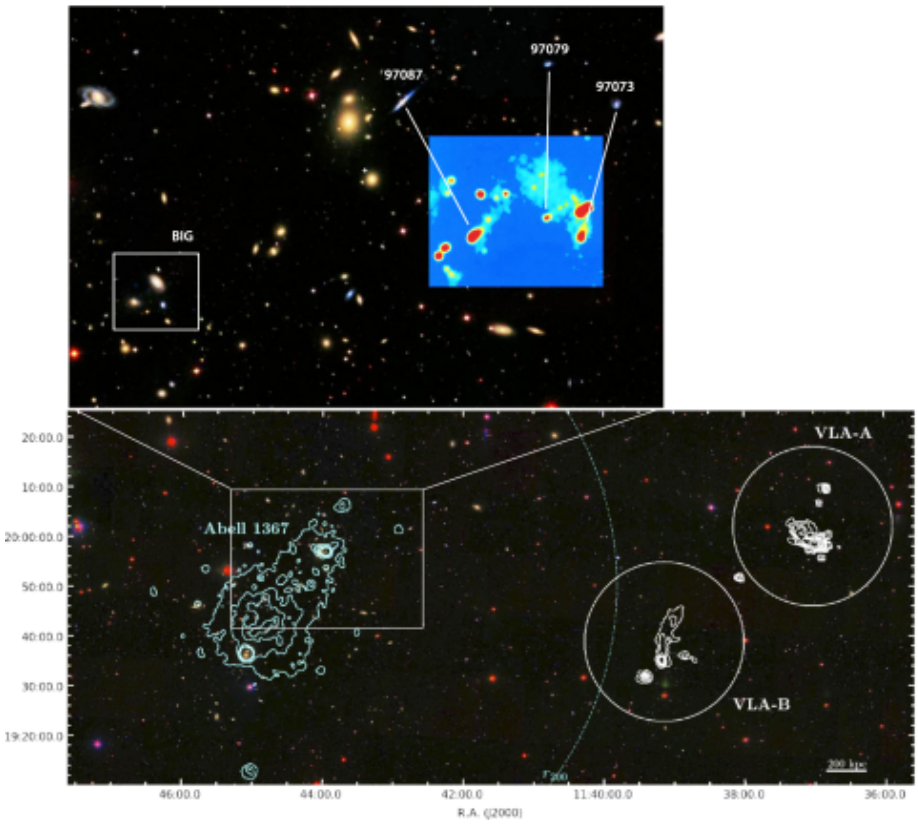

Fig. 1 (*Top*) The SDSS distribution of galaxies in the central region (40 × 25 arcmin) of A1367. *Boxes* highlight galaxies showing evidence of high-velocity first pass through the cluster IGM. The *color inset* contains a 1.4 GHz VLA continuum map showing extended trailing emission behind three galaxies CGCG 97073, 97079 and 97087 (adapted from Gavazzi et al. 1995). The *rectangle labeled* BIG lies close to the X-ray cluster center. It contains a compact group of galaxies infalling onto the cluster (Cortese et al. 2006a, b). (*Bottom*) The head-tail galaxy FGC1287 (VLA-B) and CGCG 97026 (VLA-A) are found just outside one virial radius of A1367 (adapted from Scott et al. 2012). X-ray emission (ROSAT) from the hot ICM is indicated with cyan contours. Reproduced with permission of Oxford University Press

The striking new feature of A1367 is the discovery by Scott et al. (2012) of two "HI head-tail" galaxies FGC1287 and CGCG 97026 at the cluster periphery (just outside the virial radius) reproduced in Fig. 1. This is perhaps not too surprising, as recent hydrodynamical simulations (Tonnesen & Bryan 2009; Bahe et al. 2013; Cen et al. 2014) claim that ram-pressure is effective out to 2–3 times the virial radius of a cluster. Moreover Book & Benson (2010), confirmed by observational studies of satellite galaxy SFR versus clustercentric radius, suggest that quenching of the SFR relative to the field takes place at similarly large clustercentric projected distances (Balogh et al. 2000; Verdugo et al. 2008; Braglia et al. 2009). Moreover, there is evidence that ram pressure becomes effective at lower density than previously assumed (Bekki 2009). See, for example, Freeland et al. (2010) who studied the effects of the IGM in the poor group NGC4065 belonging to the Coma supercluster, visible just 4° to the E of A1367 in Fig. 2. FGC1287 ($M_{\rm star} \sim 10^{9.9}$ $M_{\odot}$) lies a little over one virial radius away from the cluster center, i.e. approximately one Mpc away from the hot gas

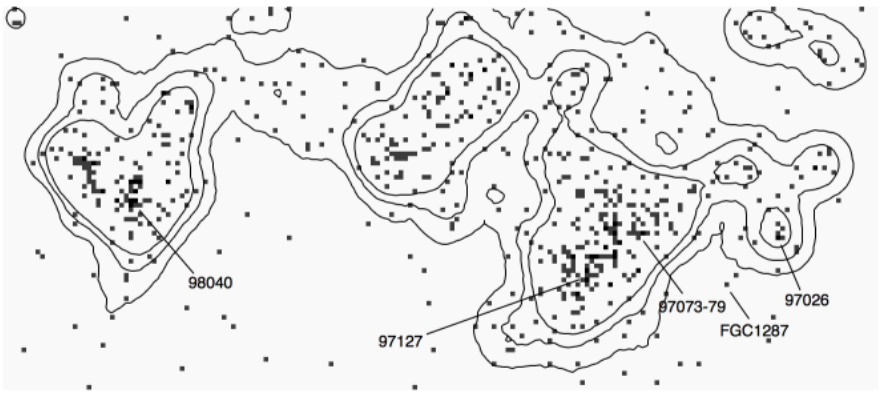

Fig. 2 Contours of the smoothed density distribution of SDSS galaxies in a $9 \times 3.5^{\circ}$ region around A1367. The large-scale distribution of galaxies in the Coma supercluster form a connected structure elongated in the E–W direction. Galaxies 97073 and 97079 (with radio and Hα tails) and the head–tail radio galaxy 97127 near the center of the main cluster are highlighted. The location of the newly discovered HI head–tail galaxies FGC 1287 and CGCG 97026 at the W periphery of the cluster are also marked, as well as the wide-angle tail CGCG 98040 (in the NGC 4065 group at the E of the cluster)

in A1367, as mapped by *ROSAT*. We remind, however, that the map reproduced in Fig. 1 underestimates the real extent of the X-ray emission from A1367, as a deeper *XMM*-Newton observation reveals (Finoguenov private communication). Environmental effects (gas deficiency and star-formation quenching) in the Virgo cluster are detected more than one virial radius away from M87 (Gavazzi et al. 2012).

It is difficult to disentangle whether the HI-tail of FGC1287 is triggered by the IGM associated with A1367 or with its hosting group. Looking at the smoothed distribution of SDSS galaxies shown in Fig. 2 it appears that galaxies around A1367 form a continuum structure with contiguous groups, elongated in the E–W direction generally traced by the Coma Supercluster as a whole. One group to the W contains 97026, the newly discovered HI tail, and another group to the E (NGC4065) contains a well-known wide-angle radio galaxy associated with 98040 (Jaffe & Gavazzi 1986).

What is perhaps more surprising is that even evolved clusters like Coma, as soon as their galaxies are observed with sufficiently long exposures, reveal the presence of trailing emission (star-forming trails or ionized gas) (Yagi et al. 2010; Yoshida et al. 2012; Fossati et al. 2012), witnessing profound ongoing environmental transformations affecting many dwarf and some massive LTGs.

Summarizing, adding the aforementioned cases to other well-known examples in the Virgo cluster (e.g. Vollmer et al. 2001) there is multiple evidence that today's clusters harbor many actively star-forming galaxies in their first-time high-velocity pass through the dense and hot IGM. Our aim is to show that they are being quickly transformed into passive systems under the influence of the dynamical pressure. We notice that most of them

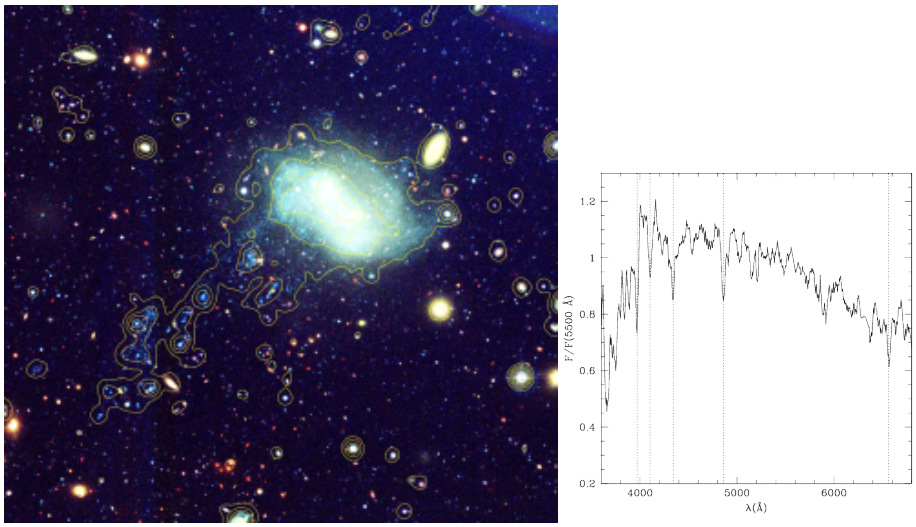

Fig. 3 *Left panel* RGB image of VCC1217 in the Virgo cluster obtained with u, g, i NGVS images with superposed contours obtained combining two long *GALEX* NUV exposures of 16,000 and 4,500 s, respectively. The integrated spectrum of the galaxy (*right panel*) is typical of a post-starburst

have stellar masses $M_{\rm star} \lesssim 10^{10}$ M$_\odot$, which is tentatively assumed hereafter as an empirical separation between dwarf and giant galaxies.

Dwarf galaxies, the most common objects in the universe, have a very important role for understanding the processes that gave birth to the local evolved stellar systems. Models of galaxy evolution consistently indicate that they are the building blocks of massive objects, formed by subsequent merging events. Only recently these objects became accessible to systematic observations outside the Local Group. Given their shallow potential wells, these "fragile" stellar systems provide us with a sensitive probe of their environment. Up to approximately 10 years ago, dwarf galaxies were supposed to belong to two main sequences: Magellanic Irregular (Im) and blue-compact-dwarf (BCD), actively star forming, dominating the field on one hand, and quiescent dwarf elliptical (dE) and spheroidal (dS0), abundant in clusters on the other. The advent of large panchromatic and kinematic surveys allowed us to realize that some Im found in clusters are in fact completely quiescent. An example is VCC1217 (IC1318) (see Fig. 3), located approximately 1.5° south of M87 in the Virgo cluster. In this dwarf ($M_{\rm star} \sim 10^{8.9}$ M$_\odot$) irregular LSB galaxy the star formation is absent from the disk, being probably truncated recently, as testified by its PSB-like spectrum. This object received recent attention due to the presence of a long tail of star-forming blobs first revealed by *GALEX*, and trailing behind it, a clear signature of an ongoing ram-pressure stripping event (Hester et al. 2010; Fumagalli et al. 2011; Kenney et al. 2014).

On the other hand, only a minority of dEs can be recognized as the low-mass counterparts of giant elliptical galaxies. Some have a complex morphology (e.g. pseudobulges, inner disks, spiral arms), some rotate (Toloba et al 2009; 2011; 2012), some contain dust, gas, and star formation in their center. Recent observations (Boselli et al. 2008a,b; Gavazzi et al. 2010) suggest that dEs, and ultimately the faint-end of the red sequence, can result from the recent migration of faint star-forming galaxies through the "green-valley". This is sketched for the Virgo cluster on the color–stellar mass relation shown in Fig. 18 using the most recent spectrophotometric models for the evolution of galaxies in rich environments. Two

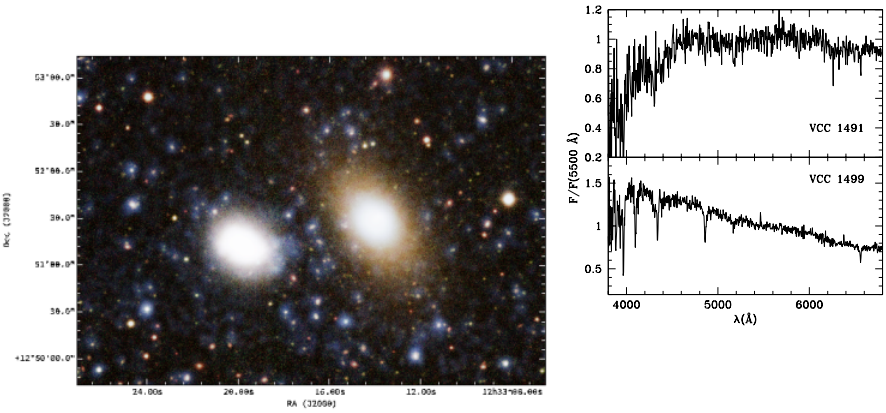

Fig. 4 *Left panel* RGB image of VCC1491 (*right-red*) and VCC1499 (*left-blue*) in the Virgo cluster obtained combining UV and optical NGVS images. Their integrated spectra (*right panel*) are characteristic of a red, passive galaxy (VCC1491, *top*) and of a PSB (VCC1499, *bottom*)

such cases are offered by VCC1491 and VCC1499 reproduced in Fig. 4. They are located within 1° projected distance from M87 in the Virgo cluster. Seen on the exquisite B-band photographic plate taken by Binggeli et al. (1985) for the construction of the Virgo Cluster Catalog (VCC) they look morphologically identical and they were both classified as dEs. In spite of their similar stellar mass [$M_{\rm star}(1491) = 10^{8.62}$ M$_\odot$, $M_{\rm star}(1499) = 10^{8.23}$ M$_\odot$], when seen on multiband CCD images they appear dramatically different in color: $(g-i)_{1491} = 1.06; (g-i)_{1499} = 0.59$, and spectroscopically (see Fig. 4, right panel). While VCC1491 has a spectrum typical of a passive galaxy, VCC1499 has a post-star-burst (PSB) spectrum (both spectra are integrated over the whole galaxy). Unfortunately for neither galaxies kinematical measurements are available, but we would not be surprised if VCC1499 was a fast rotator (Cappellari et al. 2011b), i.e. a LTG recently converted into a ETG.

Boselli et al. (2008a) and Gavazzi et al. (2010) argued that PSB (or $k+a$) galaxies (Poggianti et al. 2004) showing the characteristic blue continuum and strong Balmer lines in absorption might consist of galaxies undergoing the fast transition across the "green valley" due to an abrupt truncation of the SFR by ram-pressure. As remarked by these authors they come exclusively under the form of dwarfs (i.e. with stellar masses $M_{\rm star} \lesssim 10^{10}$ M$_\odot$) in the outskirts of local rich clusters of galaxies. The present paper is conceived for reviewing the works done in the past decade on galaxy evolution in relation to the environment (we apologize for the missing references). We hope this primarily observational review will contribute at convincing the reader that environmental transformations should be taken into higher consideration as drivers of galaxy evolution. The advent of large-scale cosmological simulations including "gastrophysics" will allow to constrain the environmental effects in detail from a theoretical point of view as well, complementing the more acknowledged stellar and AGN feedback processes. Here we will skip a detailed discussion on the physical processes, as they were extensively treated in Boselli & Gavazzi (2006). We will focus instead mainly on observations (Sects. 2, 3) leaving some room for comparison with models (Sects. 4, 5) and concluding with evidences of evolution as a function of lookback time and density.

2 Recent blind and pointed surveys of nearby clusters

2.1 Large-scale surveys

The study of environmental effects on the evolution of galaxies took advantage from several recent multifrequency surveys covering large portions of the sky.[1] Among these the one that had certainly the major impact is the SDSS (York et al. 2000). Thanks to its photometric and spectroscopic mode in the optical domain, the SDSS allowed the observation of millions of galaxies in a vast luminosity interval, located in regions spanning a wide range of environments, from local voids to the core of the richest clusters.

Early SDSS releases have been used to study the dependence of the structural, spectrophotometric, and star-formation properties of galaxies as a function of galaxy density, resulting, however, in controversial results on the role of the environment on galaxy evolution. On the one hand Kauffmann et al. (2004) found that "For galaxies in the range $10^{10} - 3 \times 10^{10} M_{\odot}$ the median specific star-formation rate decreases by more than factor of 10 as the population shifts from predominantly star-forming at low density to predominantly inactive at high densities". Conversely Hogg et al. (2004), beside confirming the morphology-density effect, do not find any further environmental difference once ETGs are separated from LTGs on the basis of their Sersic index.[2] Similarly, Balogh et al. (2004) do not see a progressive reddening of galaxies as a function of local density. In other words, they do not find evidence for objects crossing the green valley in their way from the blue to the red sequence.

The DR7 of the SDSS was released in 2009 (Abazajian et al. 2009) and included the complete photometry in the northern galactic cap; the DR9 came out in 2012 (Ahn et al. 2012) based on a new photometric pipeline; the DR10 in 2013 (Ahn et al. 2014), based on a renewed spectral pipeline. We remind that the SDSS spectral database is complete to $r = 17.77$ mag (Strauss et al. 2002), except for "shredding" and fiber conflict effects (Blanton et al. 2005a,b). To avoid large galaxies whose photometry is uncertain because of these problems, most statistical studies that came out from the SDSS are limited to $z > 0.05$. Other authors made a different use of the SDSS data: by directly analyzing the images and extracting magnitudes by hand, independently of the SDSS pipeline. With this approach Gavazzi et al. (2010, 2012, 2013a) took advantage of the SDSS superior material to directly compare the properties of galaxies in the centers of Coma, A1367, and Virgo with their isolated counterparts taken in the outskirts of these clusters.

The *GALEX* mission (Martin et al. 2005) covered the entire sky in the far (FUV, $\lambda_{\rm eff}$ 1,539 Å) and near ultraviolet (NUV, $\lambda_{\rm eff}$ 2,316 Å) down to a limit of $\simeq$21 mag with an angular resolution of $\sim$5 arcsec. Sensitive to the emission of the youngest stars, *GALEX* provided the census of the star-formation activity in galaxies in the local universe. The sensitivity of the instrument in targeted observations combined with its large field of view ($\sim$1 deg^2) allowed the detection of low surface brightness systems such as dwarf galaxies and tidal streams in several nearby clusters, making it an ideal instrument for the study of the effects of the environment in the local universe (Gil de Paz et al. 2007; Boselli et al. 2014a,b).

[1] Most large-scale surveys are currently available for the northern hemisphere. However, several large survey of the southern sky are under way, e.g. the ESO/VST and the DES (Dark Energy Survey) at NOAO.

[2] The absence of a significant environmental effect in Hogg et al. (2004) is due to a sensitivity bias: their analysis includes galaxies brighter than $M_i = -20$, while significant environmental issues affect galaxies fainter than $M_i = -19$.

The gaseous component, primary feeder of the star-formation process, was observed thanks to the Arecibo Legacy Fast Arecibo L-band Feed Array (ALFALFA),[3] first announced by Giovanelli et al. (2005) and completed in 2012. This survey has mapped ∼7,000 deg^2 of the high galactic latitude sky visible from Arecibo (i.e in the declination strip 0°–30°), providing a HI line spectral database covering the redshift range between −1,600 km s^{-1} and 18,000 km s^{-1} with 5 km s^{-1} resolution at a sensitivity of 2.3 mJy. Exploiting Arecibo's large collecting area and relatively small beam size (3.5′), ALFALFA was specifically designed to probe the faint end of the HI mass function in the local universe down to M(HI) $\simeq 10^7$ M$_\odot$ (Martin et al. 2010). Haynes et al. (2011) presented the current catalog of 21 cm H I line sources extracted from ALFALFA over ∼2,800 deg^2 of sky: the α.40 catalog. Covering 40 % of the final survey area, the α.40 catalog contains 15,855 sources in the spring sky, in two declination strips: 4°–16° and 24°–28°. These include large stretches of the Local and of the Coma superclusters.

In the infrared domain, the all sky surveys undertaken with the *AKARI* (Murakami et al. 2007) and *WISE* (Wright et al. 2010) space missions provided photometric data for hundreds of thousands of galaxies in the spectral range 2–180 μm. With a significantly better sensitivity and angular resolution than *IRAS*, *AKARI* and *WISE* are crucial for quantifying the contribution of the old stellar populations dominating the emission of galaxies for $\lambda \lesssim 5$ μm and that of the warm and cold dust components at longer wavelengths. Dust emission is critical for quantifying the attenuation of the stellar light in the UV and optical domain and is thus crucial for a correct determination of the present and past star-formation activity of galaxies.

2.2 Blind panoramic surveys of clusters at $z = 0$ and their host superclusters

Because of the limited sensitivity of the instruments used in all sky surveys, the study of the dwarf galaxy population was mainly restricted to the very nearby universe. Different representative regions have been the target of dedicated studies. Among these, the most studied are certainly the Virgo and the Coma clusters. The Virgo cluster is the largest concentration of galaxies within 35 Mpc. Virgo is one of the closest rich clusters, whose distance (of only 16.5 Mpc, Gavazzi et al. 1999; Mei et al. 2007) allows us to study galaxies spanning a wide range in morphology and luminosity, from giant spirals and ellipticals down to dwarf irregulars, BCDs, dEs, and dS0. Furthermore, Virgo is still in the process of being assembled so that a wide range of processes (ram-pressure stripping, tidal interactions, harassment, and pre-processing) are still taking place. The Virgo cluster has been the target of several blind multifrequency surveys covering the whole range of the electromagnetic spectrum. The *GALEX* UV Virgo Cluster Survey (GUViCS; Boselli et al. 2011)[4]. covered ≃120 deg^2 centered on the cluster in the FUV and NUV bands providing UV data for more than 1,200,000 sources, out of which ∼850 identified as cluster members (Voyer et al. 2014; see Fig. 5). The sensitivity of the survey, reached typically with ∼1,500 s (one orbit) exposures, allowed the detection of low surface brightness features of 27.5–28 mag arcsec^{-2} such as dwarf galaxies, including quiescent systems (Boselli et al. 2005a) and tidal features produced during the mutual interaction of galaxies (Boselli et al. 2005b; Arrigoni Battaia et al. 2012). The UV observations are of paramount importance for a large number of studies. In star-forming galaxies, the present day star-formation activity can be measured from the UV

[3] http://egg.astro.cornell.edu/index.php/.
[4] http://galex.lam.fr/guvics/

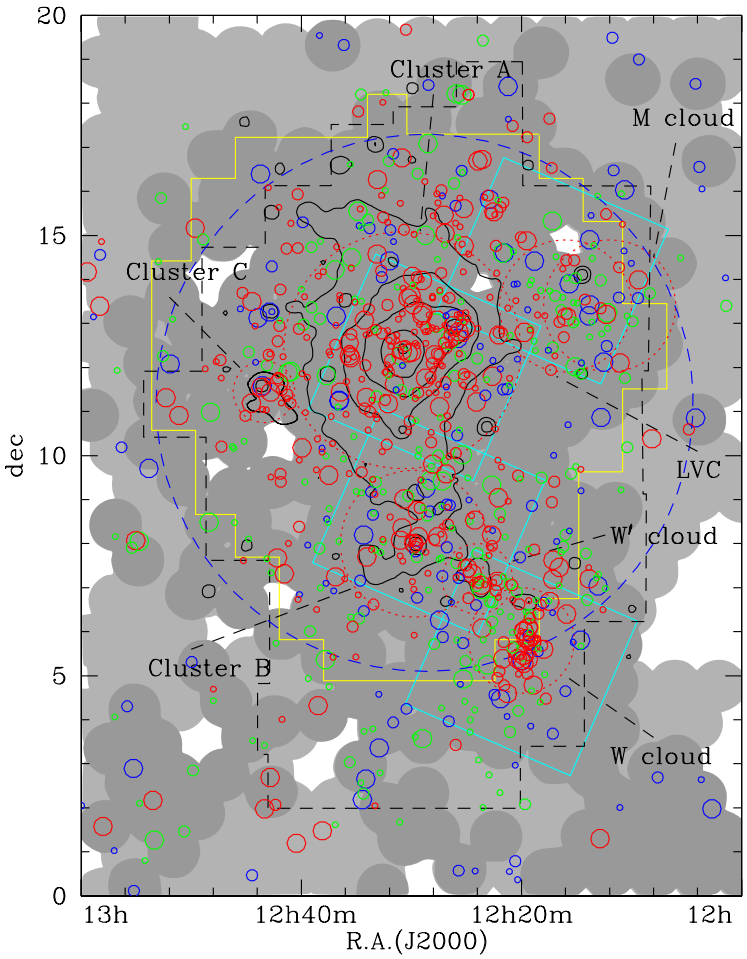

Fig. 5 Coverage of different surveys of the Virgo cluster region in between 12 h < R.A.(J2000) < 13 h and 0° < dec < 20°. The footprint of the Virgo Cluster Catalogue (VCC, Binggeli et al. 1985) is indicated by the *black dashed line*, the Next Generation Virgo Cluster Survey (NGVS, Ferrarese et al. 2012) by the *yellow solid line*, and the *Herschel* Virgo Cluster Survey (HeViCS, Davies et al. 2010) by the *cyan solid line*. The *light and dark gray areas* indicate the regions observed during the *GALEX* Ultraviolet Virgo Cluster Survey (GUViCS, Boselli et al. 2011) in the NUV (2,316 Å) band at two different depths (adapted from Boselli et al. 2014a). *Red, green, and blue empty circles* indicate Virgo cluster galaxies belonging to the red sequence, green valley, and blue cloud. The *size of the symbols* is proportional to the galaxy stellar mass. The *black contours* indicate the X-ray diffuse emission of the cluster, from Böhringer et al. (1994). Courtesy of ESO

flux emitted by the youngest stellar population (Kennicutt 1998; Boselli et al. 2001, 2009), provided that dust extinction can be accurately determined (e.g. using the far-IR to UV flux ratio, Cortese et al. 2006a, 2008a; Hao et al. 2011). In quiescent galaxies, the UV emission can help to date the last generation of stars (on a few 100 Myr timescale) or is associated to very old populations (UV upturn; O'Connell 1999; Boselli et al. 2005a).

The Virgo cluster has been mapped in four optical bands (u^*, g', i', z') by the Next Generation Virgo cluster Survey (NGVS, Ferrarese et al. 2012).[5]. Carried out with the 1 deg^2 MegaCam instrument on the Canadian French Hawaii Telescope, the survey covered 104 deg^2 of the Virgo cluster, from the dense core out to the virial radius (see Fig. 5). Designed to study at the same time point-like and extended, low surface brightness sources, it has a sensitivity of 25.9 g magnitudes for point-sources and a surface brightness limit of μ_g 29 mag arcsec^{-2}. The survey has detected $\sim 3 \times 10^7$ sources, including hundreds of low surface brightness Virgo cluster members down to absolute magnitudes of $M_{\rm g} \sim -6$, and thousands of globular clusters associated with the massive galaxies. Sensitive to the stellar emission, the survey has been designed to study the luminosity and mass function of cluster galaxies, as well as the color–magnitude and the most important structural and photometric scaling relations down to this absolute magnitude limit.

The Virgo cluster has been observed in the far infrared by *Spitzer* and *Herschel*. The VIRGOFIR program (Fadda et al., in prep.) mapped 30 deg^2 of the Virgo cluster at 24 and 70 μm with *Spitzer*, while the *Herschel* Virgo Cluster Survey (HeViCS; Davies et al. 2010, 2012)[6]. 64 deg^2 with PACS (100, 160 μm) and SPIRE (250, 350, 500 μm) on board of *Herschel* (see Fig. 5). The HeViCS survey is confusion limited at 250 μm ($\sim$1 MJy sr^{-1}) and has an angular resolution spanning from 6″ at 100 μm up to 36″ at 500 μm (diffraction limited). It is thus perfectly suited for studying the cold dust properties, one of the most important phases of the ISM in galaxies. Far infrared data are fundamental for accurately correcting for dust attenuation the UV and optical emission of galaxies and are thus crucial for quantifying and studying the present day star-formation activity, and the past star-formation history of cluster galaxies.

At the distance of the Virgo cluster the ALFALFA survey provided HI masses for galaxies down to M(HI) $\simeq 10^{7.5}$ M$_\odot$ (Giovanelli et al. 2007; Kent et al. 2008; Haynes et al. 2008). Slightly deeper HI data (M(HI) $\simeq 10^7$ M$_\odot$) have been obtained by the Arecibo Galaxy Environment Survey (AGES; Taylor et al. 2012, 2013) on the cluster along two radial strips covering M49 (10×2 deg^2) and east of M87 (5 deg^2). Finally, X-ray data relative to the emission of the hot ICM are available thanks to *ROSAT* (Böhringer et al. 1994) and *ASCA* (Shibata et al. 2001), including spectroscopy from *XMM*-Newton (Urban et al. 2011).

The Coma cluster has also been the target of several multifrequency blind surveys (see Fig. 6). Located at a distance of $\sim$96 Mpc, Coma is a relaxed, spiral poor cluster characterized by a strong X-ray emission (Sarazin 1986; Briel et al. 2001). Nine square degree of the cluster, corresponding to $\sim$25 Mpc^2, have been observed in the UV with *GALEX* by Cortese et al. (2008b), and one extra field centered on the infalling region 1.6 Mpc southwest from the cluster core with a deep observation by Hammer et al. (2010a), and another one by Smith et al. (2010) centered on the cluster core. The Coma cluster has been also the target of a dedicated *Hubble*/ACS blind survey designed to cover 740 arcmin^2 but unfortunately not completed because of the failure of the ACS camera (Carter et al. 2008a; Hammer et al. 2010b).[7]. The central 4 deg^2 of the Coma cluster have been observed in the infrared domain by *Spitzer* at 24 and 70 μm (Bai et al. 2006). The Coma cluster is also included in the H-ATLAS survey (Eales et al. 2010)[8]. and has thus been observed by *Herschel* at low sensitivity (5σ sensitivity for point-like sources $\simeq$50 to 100 mJy) in the PACS and SPIRE bands at 100, 160, 250, 350, and 500 μm. The cluster has been also the target of a deeper,

[5] https://www.astrosci.ca/NGVS/The_Next_Generation_Virgo_Cluster_Survey/Home.html

[6] http://wiki.arcetri.astro.it/bin/view/HeViCS/WebHome

[7] http://astronomy.swin.edu.au/coma/index-mm.htm

[8] http://www.h-atlas.org/

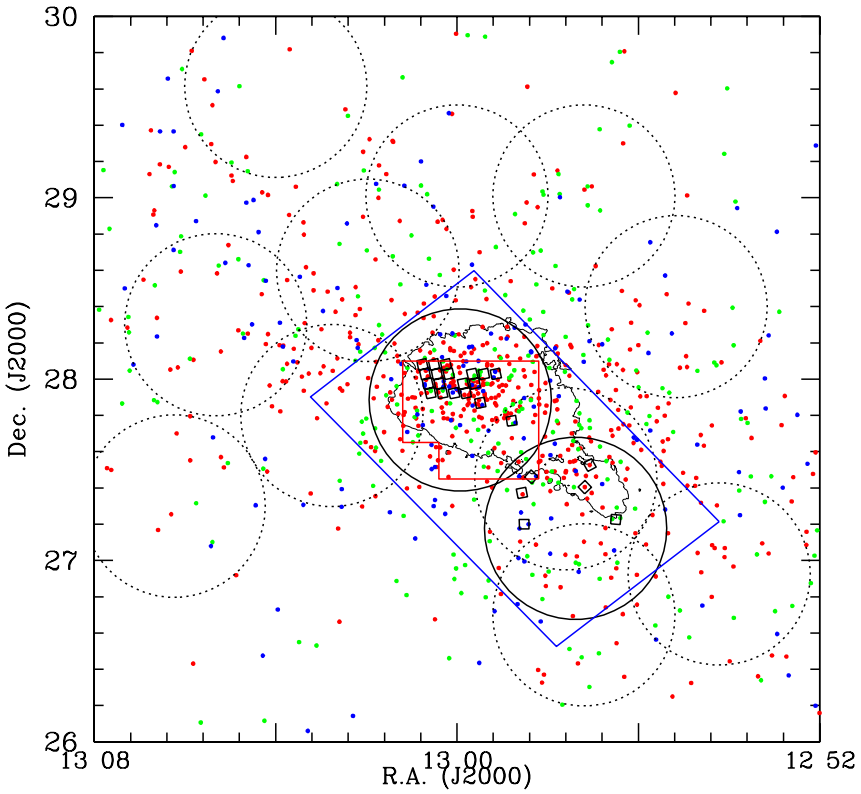

Fig. 6 Coverage of available surveys in the Coma cluster region. The deep *GALEX* fields centered on the core of the cluster (Smith et al. 2010) and on NGC 4839 (Hammer et al. 2010b) are indicated with large (1 deg diameter) *solid circles*, the shallower one obtained by Cortese et al. (2008b) with *dotted circles*. The *blue rectangle* indicates the area covered with *Herschel* by Hickinbottom et al. (2014). The *red polynomial* region centered on the core of the cluster shows the area covered by deep H_α observations of Yagi et al. (2010). The footprints of the ACS Coma survey (Carter et al. 2008a) are indicated by *small squares*. *Red*, *green*, and *blue dots* indicate SDSS galaxies belonging to the red sequence, green valley, and blue cloud. The lowest contour of the X-ray emission from XMM is given. The patchy black contur in the center of the image shows the X-ray emission of the hot IGM (Briel et al. 2001)

dedicated observation with *Herschel*/PACS at 70, 100, and 160 μm on an area of $1.75 \times 1.0^\circ$ encompassing the core and the southwest infalling region (Hickinbottom et al. 2014). Spectroscopic observations of dwarf galaxies in the Coma cluster have been also obtained by Smith et al. (2008, 2009). Worth mentioning are also the impressive narrow band Hα imaging observations of large portions of the Coma cluster done with the Suprime-Cam on the Subaru telescope by Yagi et al. (2007, 2010) and Yoshida et al. (2008) and the following spectroscopic observations of Yoshida et al. (2012). We remind that X-ray data of the cluster are available thanks to *ROSAT* (Briel et al. 1992), *XMM* (Briel et al. 2001; Arnaud et al. 2001; Neumann et al. 2001; Finoguenov et al. 2004a), *Chandra* (Vikhlinin et al. 2001; Churazov et al. 2012; Andrade-Santos et al. 2013), and *INTEGRAL* (Renaud et al. 2006; Eckert et al. 2007).

Other recent blind surveys of very nearby clusters worth mentioning are those of A1367 in the UV and HI bands (Cortese et al. 2005, 2008a,b), of the Shapley supercluster in the optical (Mercurio et al. 2006), near-infrared (Merluzzi et al. 2010), far infrared and UV bands (Haines et al. 2011), including optical spectroscopy (Smith et al. 2007), and X-ray (Bonamente et al. 2001; Akimoto et al. 2003; Finoguenov et al. 2004b), and of the Fornax cluster in the PACS and SPIRE *Herschel* bands (Davies et al. 2013), and in X-ray by *XMM* (Murakami et al. 2011), while a ultra deep optical survey (FOCUS) is under way.

2.3 Pointed observations

In the recent years a growing effort has been also devoted in targeted multifrequency observations of nearby cluster and field galaxies, including dwarfs, with the specific purpose of understanding the physical processes at the origin of the red sequence in high-density regions. A particular attention has been paid in gathering high-resolution spectroscopy data necessary to constrain the kinematical properties of the observed galaxies. The SMAKCED (Stellar content, Mass and Kinematics of Cluster Early-type Dwarfs) project (Janz et al. 2012)[9]. has been designed to obtain medium resolution (R = 3,800), long slit spectroscopy and deep near infrared photometry of ∼100 dwarf elliptical galaxies in the Virgo cluster. This project is a continuation of the study of the kinematic and spectrophotometric properties of dE started a few years before within the MAGPOP collaboration by Toloba and collaborators (Toloba et al. 2009, 2011, 2012). The ATLAS^{3D} survey (Cappellari et al. 2011a),[10]. although limited to relatively massive objects ($M_{\rm star} \gtrsim 6 \times 10^9$ M$_\odot$), was designed to observe with SAURON on the William Herschel Telescope a volume limited sample ($D < 42$ Mpc) of 260 ETGs in the local universe using kinematic and spectrophotometric data at different frequencies. The ATLAS^{3D} survey, which was originally defined to study 2D intermediate resolution spectroscopy data, extended in data quality and in statistics the SAURON project (Bacon et al. 2001). Another recent survey of nearby galaxies based on 2D-integral field spectroscopy at intermediate/low resolution (R 850 and 1,650 in the spectral range 3,700–7,000 Å) data is CALIFA (Calar Alto Legacy Integral Field Area survey; Sanchez et al. 2012),[11]. a project designed to observe with PPAK at the 3.5-m telescope of Calar Alto and study ∼600 galaxies in the local universe ($0.005 < z < 0.03$). Although mainly limited to massive galaxies, the sample includes galaxies spanning a wide range in morphological type and environment, including Coma and A1367, and is thus perfectly suited to study any pos-

[9] http://smakced.net/

[10] http://www-astro.physics.ox.ac.uk/atlas3d/

[11] http://califa.caha.es/

sible physical process able to transform star forming into quiescent systems in high-density regions.

High-quality optical images of dwarf elliptical galaxies in the Virgo cluster have been obtained with the ACS camera on the *HST* during the ACS Virgo cluster survey (ACSVCS; Cote et al. 2004).[12]. The survey covered 100 ETGs, out of which 35 dE, dEN or dS0, in the F475W and F850LP bandpasses, which roughly correspond to the SDSS g and z bands. The same team has also undertaken the ACS Fornax cluster survey (ACSFCS; Jordan et al. 2007a,b), a similar survey of 43 ETGs in the Fornax cluster. In the optical domain it is worth mentioning Hα3, a narrow-band Hα imaging survey of dwarf, HI-detected star forming galaxies located in the surrounding regions of the Virgo and Coma/A1367 clusters (Gavazzi et al. 2012, 2013a,b). This survey extended previous observations of the clusters (Gavazzi et al. 1998, 2002, 2006a; Koopmann et al. 2001; Boselli et al. 2002; Boselli & Gavazzi 2002) to objects in low density regions at similar distances. Concerning the gaseous component we should mention the VLA survey of Virgo galaxies (VIVA) of Chung et al. (2009) that, although targeting bright spirals, allowed the detection of extraplanar HI gas stripped during the interaction with the hot ICM (Chung et al. 2007) where local episodes of star formation can give birth to new dwarf systems (see Sect. 3.8). We must also mention the *Herschel* Reference Survey (HRS; Boselli et al. 2010),[13] a project aimed at studying among other scientific topics, the effects of the cluster environment on the properties of the ISM in galaxies. Multifrequency data covering the whole electromagnetic spectrum, including new *Herschel* data, have been collected in the literature or thanks to dedicated observations. The sample is ideally designed for this purpose since it is a complete volume-limited ($15 < Dist < 25$ Mpc), K-band-selected sample of galaxies spanning a wide range in morphological type, including at the same time field objects and Virgo cluster galaxies selected using consistent criteria. As selected, the sample includes spiral galaxies down to $M_{\rm star} \simeq 3 \times 10^8$ M$_\odot$ and thus covers the relatively bright dwarf systems.

3 Main observational results

3.1 Luminosity functions

The availability of large-scale multifrequency surveys such as SDSS and *GALEX* allowed the determination of the luminosity function in different photometric bands and the study of the variation of their characteristic parameters as a function of galaxy density (e.g. Blanton & Moustakas 2009). With respect to previous works for the major part based on the observations of the central regions of a few well-known clusters, these surveys have the advantage of extending the study to the periphery of the cluster, not always mapped by pointed observations. These regions are of great importance since they define the prevailing conditions first encountered by galaxies infalling in high-density regions (e.g. Boselli & Gavazzi 2006). Owing to the unprecedented statistical significance of datasets extracted from the SDSS, the role of the environments on the evolution of galaxies belonging to regions of different density, from the field to loose and compact groups up to massive clusters, has been significantly clarified.

By combining SDSS data of 130 X-ray selected clusters at $z \simeq 0.15$ (Popesso et al. 2005) determined and studied the properties of the composite luminosity functions of nearby clusters. This work has shown that the luminosity function has a bimodal behavior, with an

[12] https://www.astrosci.ca/users/VCSFCS/Home.html
[13] http://hedam.lam.fr/HRS/

upturn and an evident steepening in the faint magnitude range in any SDSS band. Both the bright and the faint end can be fitted with a Schechter function, the former with a slope $\alpha \simeq -1.25$, the latter with $-2.1 \leq \alpha \leq -1.6$ (see Fig. 7). The same authors were also able to separate the contribution of early- and late-type galaxies using color indices (Popesso et al. 2006). They have shown that while the luminosity function of late-type systems can be fitted with a single Schechter function of slope $\alpha = -2.0$ in the r-band, the early-types require two Schechter functions, the faint one being responsible for the faint-end upturn observed in the global composite luminosity function of the cluster. The shape of the bright-end tail of the early-type luminosity function does not depend on the local galaxy density, while the faint-end shows a significant and continuous variation with the environment, with a clear flattening near the core of the cluster. A steepening of the faint-end of the luminosity function at the periphery of nearby clusters and a flattening in the core has been also observed by Barkhouse et al. (2007, 2009) using data on 57 low-redshift Abell clusters observed with the KPNO 0.9 m telescope. All these teams interpreted these results as an evidence of a combined effect of galaxy transformation from star forming to quiescent systems through harassment in the periphery and dwarf tidal disruption in the core (Popesso et al. 2006; Barkhouse et al. 2007; de Filippis et al. 2011). The presence of an upturn at faint magnitudes in the luminosity function, however, was questioned by de Filippis et al. (2011), while a significantly flatter faint end slope ($\alpha \sim -1.1$) has been found in the Hydra I and the Centaurus clusters down to $M_V \sim -10$ by Misgeld et al. (2008, 2009). Hansen et al. (2009) have shown that the shape of the luminosity function of satellites does not change with clustercentric distance. They have also shown that the luminosity function of both red and blue satellites is only weakly dependent on richness. Their ratio, however, dramatically changes. The average color of satellites is redder near the cluster centers.

The properties of the SDSS luminosity function of cluster galaxies was extended to groups by Zandivarez et al. (2006), Zandivarez & Martinez (2011) and Robotham et al. (2010). Zandivarez et al. (2006) and Zandivarez & Martinez (2011) have shown a steepening of the faint end slope and a brightening of the characteristic magnitude as the mass of the system increases, while Robotham et al. (2010) concluded that the steepening at the faint end is mainly due to an increase of the quiescent galaxy population.

Studies of very nearby clusters such as Virgo have the advantage of both detecting the dwarf galaxy population down to much fainter limits and determine cluster memberships according to different and independent criteria such as colors, morphology, surface brightness, unpractical at larger distances. Recently, Lieder et al. (2012) determined the V and I luminosity function of the central $4\,\mathrm{deg}^2$ of the Virgo cluster, deriving a faint end slope $\alpha = -1.50$. Using new spectra of galaxies in the direction of the Virgo cluster, Rines & Geller (2008) have shown that the faint-end of the r-band luminosity function has a slope consistent with that of the field ($\alpha = -1.28$) down to $M_r \simeq -13.5 \simeq M^* + 8$, thus significantly flatter than that generally determined for clusters using SDSS data (e.g. Popesso et al. 2005, 2006; see Fig. 7). The analysis of Rines & Geller (2008) has indicated that the difference is primarily due to the use of a statistical subtraction for the correction of the background contamination. They have shown that a simple separation in apparent magnitude versus surface brightness, originally proposed by Sandage and collaborators (Sandage et al. 1985; Binggeli et al. 1985) and later adopted by Boselli et al. (2011) in the UV bands, provides a powerful membership classification. They thus opened new ways for identifying cluster members, allowing the determination of the optical luminosity function in five photometric bands down to $M_g \simeq -6(M^* + 15)$ on a region centered on the Virgo cluster as large as $104\,\mathrm{deg}^2$ using the NGVS data (Ferrarese et al. 2012). The preliminary results obtained using the NGVS data of the central $4\,\mathrm{deg}^2$ of Virgo seem to indicate that the optical luminosity function of Virgo

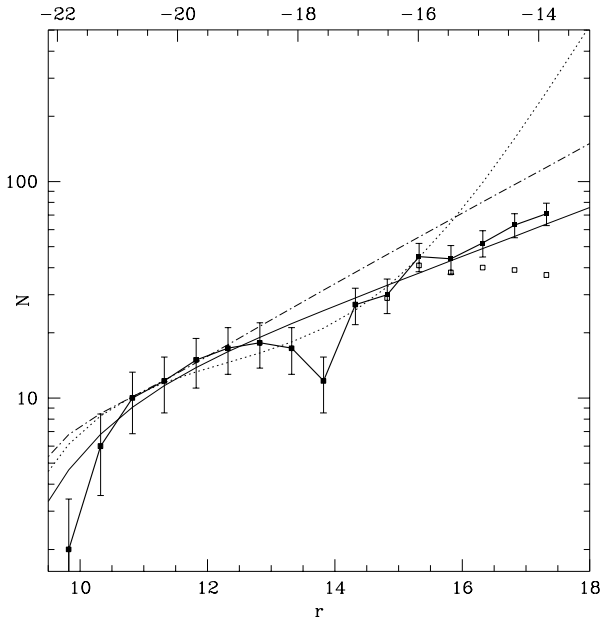

Fig. 7 The r band luminosity function of the Virgo cluster within 1 Mpc from M87, from Rines & Geller (2008) (*filled squares*) (*upper* (*lower*) scale r absolute (apparent) magnitude). The fitted Schechter function (*black solid line*) is compared to the field luminosity function from the SDSS of Blanton et al. (2005b) (*dotted–dashed line*) and to the composite luminosity function of clusters of Popesso et al. (2006) (*dotted line*). The optical luminosity function of Virgo has a slope comparable to that of the field once low surface brightness objects are considered. © AAS. Reproduced with permission

has a slope of $\alpha \simeq -1.4$ down to this absolute magnitude limit (Ferrarese, private communication). We recall that this value, which perfectly matches that obtained in the eighties by Sandage and collaborators (1985) using photographic plate material, is very similar to the one obtained for the field using the SDSS once low surface brightness objects as those detected in Virgo are considered (Blanton et al. 2005b).

Pointed observations with the *GALEX* satellite allowed the determination of the UV luminosity function of well-known nearby clusters such as Coma (Cortese et al. 2008b; Hammer et al. 2012), A1367 (Cortese et al. 2005), the Shapley supercluster (Haines et al. 2011), and the Virgo cluster (Boselli et al. 2011) in two photometric bands (FUV, $\lambda_{\rm eff}$ = 1,539 Å; NUV, $\lambda_{\rm eff}$ = 2,316 Å) (see Fig. 8). Steep slopes of the fitted Schechter functions ($\alpha \simeq -1.5/-1.6$) both in the NUV and FUV bands have been observed in Coma (Cortese et al. 2008b), A1367 (Cortese et al. 2005), and in the Shapley supercluster (Heines et al. 2011) down to UV absolute magnitudes of $\simeq$−14. These values of α are significantly steeper than those observed in the field by (Wyder et al. 2005; $\alpha \simeq -1.2$). By dividing galaxies according to their morphological type, these authors have also shown that the steepening of the observed UV luminosity function is due to the contribution of ETGs, becoming important at faint luminosities. We recall that in these quiescent objects the UV emission is not only related to star-forming events as in LTGs (e.g. Boselli et al. 2009), but rather to evolved stellar populations (UV upturn; e.g. O'Connell 1999; Boselli et al. 2005a). Slightly flatter slopes ($\alpha = -1.39$) have been observed in the infalling region centered on NGC 4839 in

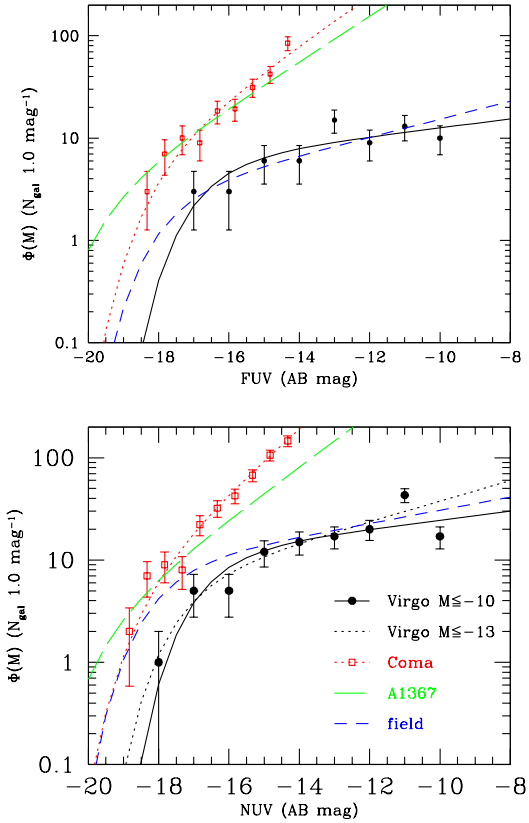

Fig. 8 The FUV (*upper panel*) and NUV (*lower panel*) luminosity functions of the Virgo cluster (*black symbols and solid line*) compared to that of the Coma cluster (*red*), A1367 (*green*), and the field (*blue*), from Boselli et al. (2011). The UV luminosity function of the Virgo cluster is similar to that of the field. Courtesy of ESO

Coma by Hammer et al. (2012) using a deep *GALEX* field including galaxies down to UV magnitudes of −10.5.

The GUViCS survey allowed the determination of the UV luminosity function down to UV magnitudes of −10 (M^*_{UV} + 7) in the central 12 deg^2 of the Virgo cluster (Boselli et al. 2011, Fig. 8). The faint-end slope of the fitted Schechter function determined in this work ($\alpha \simeq -1.1/-1.2$) is significantly flatter than the one observed in other clusters and very close to the one determined for the field. Boselli et al. (2011) interpreted the difference between the faint-end slope of the luminosity function of Virgo and other nearby clusters as due to two possible effects. The first is related to the small volume sampled by their study and thus to the small number of luminous objects used to constrain the shape of their luminosity function. They have also shown, however, that because of the higher distance of the other clusters, the determination of their luminosity functions suffers from significantly narrower dynamic range in luminosity (down to −14 vs. −10 in Virgo) and by the quite uncertain statistical

Table 1 The faint-end slope of the luminosity function.

Band		Reference	α
OPT	130 clusters	Popesso et al. (2005)	−2.0
OPT	Hydra, Centaurus	Misgeld et al. (2008, 2009)	−1.1
OPT	Virgo	Lieder et al. (2012)	−1.5
OPT	Virgo	Rines & Geller (2008)	−1.28
OPT	Virgo	Ferrarese et al. (2012)	−1.4
UV	Coma/A1367	Cortese et al. (2005)	−1.5/−1.6
UV	Shapley	Haines et al. (2011)	−1.5
UV	field	Wyder et al. (2005)	−1.2
UV	Coma (N4839)	Hammer et al. (2012)	−1.39
UV	Virgo	Boselli et al. (2011)	−1.1/−1.2
FIR	Coma	Bai et al. (2006, 2009)	−1.4/−1.5
FIR	Shapley	Haines et al. (2011)	−1.4/−1.5

corrections for the background contamination. This conclusion is consistent with the results of Rines & Geller (2008) obtained in the optical bands. The mild steepening of the faint-end of the luminosity function is primarily due to the population of evolved galaxies (E-S0-dE; Boselli et al. 2011). Given the similarity of the field and cluster luminosity functions, Boselli et al. (2011) concluded that their results are consistent with a transformation of star-forming dwarf galaxies in quiescent systems due to a ram pressure stripping event removing their gas content once galaxies fall into the cluster.

The study of the luminosity function of cluster galaxies has been extended to the far-infrared domain thanks to *Spitzer* and *Herschel*. Bai et al. (2006, 2009), using 24, 70, and 160 μm MIPS data determined the luminosity function of the two clusters Coma and A3266 ($z = 0.06$) down to $L_{\rm IR} \sim 10^{42}$ erg s^{-1} and $L_{\rm IR} \sim 10^{43}$ erg s^{-1}, respectively. These works have shown that the far-infrared luminosity function of these cluster galaxies ($\alpha = -1.4/-1.5$ and $L^* \sim 10.5 L_\odot$) is comparable to that observed in the field. They have also shown that both L^* and α fade close to the cluster core. Similar results have been obtained in the 24 and 70 μm bands by Haines et al. (2011) in the Shapley supercluster. Haines et al. (2011) interpreted these results as an evidence that the LTG population, responsible for the far-infrared emission, has been only recently accreted in clusters. More recently Davies et al. (2012) determined the first far-infrared luminosity distribution in the *Herschel* PACS (100–160 μm) and SPIRE (250–350–500 μm) bands for the central 64 deg^2 of the Virgo cluster. They have shown that optically selected galaxies have a far-infrared luminosity distribution peaked at intermediate luminosities, showing a lack of both bright and low-luminosity systems. The faint-end slope of the various luminosity functions is summarized in Table 1.

3.2 Gas content

The availability of HI blind surveys on large regions of the sky such as ALFALFA (Giovanelli et al. 2005) and AGES (Taylor et al. 2012, 2013) allowed the acquisition of homogeneous sets of data down to a well-defined sensitivity limit for extragalactic sources belonging to a large variety of environments. Indeed ALFALFA and AGES included nearby clusters such as Virgo (Giovanelli et al. 2007; Kent et al. 2008; Haynes et al. 2011), Coma and A1367 (Cortese et al. 2008c). These surveys are generally less deep than previous pointed observations of selected objects but cover simultaneously and without any a priori selection all kind of extragalactic sources. They mainly confirmed that the atomic gas content of galaxies decreases in high-density regions (e.g. Cayatte et al. 1990; Solanes et al. 2001; Gavazzi et

al. 2005, 2006b). They also allowed the detection of a minority of ETGs, including dwarf systems, inside the Virgo cluster with gas contents of the order of a few 10^7 $M_\odot$ (di Serego Alighieri et al. 2007). These surveys led to the first robust determination of the mean structural and spectrophotometrical properties of HI-selected galaxies in different environments and to compare them with those of optically selected samples (Gavazzi et al. 2008; Cortese et al. 2008c). The main contribution of these surveys to the study of the role of the environment on galaxy evolution, however, comes from the combination of HI data with optical and UV data from SDSS and *GALEX*. Using a sample of ∼10,000 objects with multifrequency data, Huang et al. (2012) have shown that, for stellar masses below $M_{\rm star} \lesssim 10^{9.5}$ $M_\odot$, galaxies follow a sequence along the color–magnitude relation (CMR) or the *SSFR* (star formation per unit stellar mass or specific star formation) vs. M_{star} relation regulated by the available quantity of HI gas, which becomes the dominant barionic component in low mass systems. By studying this effect in different environments, from the field to the core of nearby rich clusters and including groups, Gavazzi et al. (2013a,b) confirmed that the distribution of galaxies along the CMR below $M_{\rm star} = 10^{9.5}$ $M_\odot$ is regulated by their atomic gas content. Late-type galaxies located on the blue sequence have larger gas fractions than spirals in the green valley, or post starburst galaxies characterized by red colors (Boselli et al. 2014a,b). The galaxies mostly devoid of gas are the red early-type systems forming the red sequence. Gavazzi et al. (2003a, 2013b) have also shown that this sequence in colors or gas fraction is also related to the mean density of the environment where galaxies reside, with redder colors and gas-poor systems dominating high-density regions (see Fig. 9). These results, that extend previous analysis mainly based on massive galaxies (Hughes & Cortese 2009; Cortese & Hughes 2009), have been interpreted as a clear evidence that gas removal due to ram pressure stripping events quenches the activity of star formation, transforming gas-rich, star-forming systems into quiescent objects, as first proposed by Boselli et al. (2008a,b). The work of Gavazzi et al. (2013b), combined with that of Fabello et al. (2012) based on stacking analysis of HI data of a large sample of nearby low-mass galaxies and that of Catinella et al. (2013) for massive systems, however, have shown that gas removal and the relative quenching of the star-formation activity is already present in intermediate-density regions such as groups with halo masses $M > 10^{13}$ $M_\odot$.

Interestingly, all these evidences questioned the general assumption that in massive galaxies the quenching of the activity of star formation is mainly due to AGN feedback (e.g. Martin et al. 2007; Schawinski et al. 2009, see, however, Schawinski et al. 2014), proposing environmental effects as an alternative process for the origin of the green valley (Hughes & Cortese 2009; Cortese & Hughes 2009). The most recent CO surveys of cluster and field objects support this scenario. The analysis of a large K-band-selected, volume-limited sample of nearby field and cluster galaxies, the *Herschel* Reference Survey (Boselli et al. 2010), as well as the detailed study of a small sample of CO mapped galaxies, have both shown that also the molecular gas phase is stripped by the interaction of galaxies with the hot intergalactic medium permeating rich clusters such as Virgo (Fumagalli et al. 2009; Boselli et al. 2014b). The stripping process, however, is less efficient than that on the atomic phase because the molecular hydrogen is mainly located in the central regions of galaxies, where the gravitational restoring force is at its maximum. This evidence supports the idea that the responsible process for gas removal is ram pressure stripping (Fumagalli et al. 2009; Scott et al. 2013; Boselli et al. 2014b). All these works have been mostly limited to massive galaxies since the CO observation of metal-poor, low-luminosity objects is still challenging. We can expect, however, that given the shallower potential well of dwarf galaxies with respect to massive systems, the stripping of the gaseous component in all its phases is even more efficient in low-mass objects.

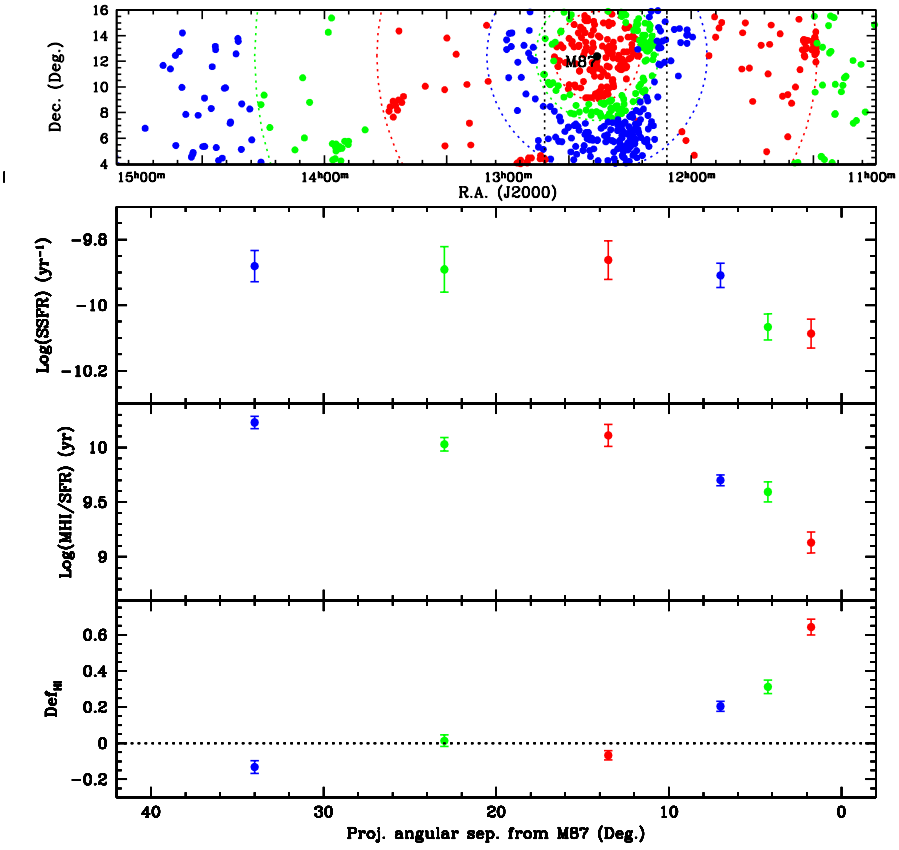

Fig. 9 *Upper panel*: the sky distribution of late-type galaxies within seven annuli of increasing radius from M87. Galaxies in each ring are given with a *different color*. Variation of the specific star formation rate *SSFR* (*middle upper*), of the HI mass per unit star formation rate *SFR* per unit HI mass (*middle lower*), and of the HI-deficiency parameter $\mathrm{Def_{HI}}$ (*lower*) as function of the projected angular separation from M87 (from Gavazzi et al. 2013a). Courtesy of ESO

The HI blind surveys of the nearby universe have also revealed the presence in clusters of HI clouds not associated with any stellar component (Kent et al. 2007, 2009; Kent 2010; Haynes et al. 2007 in ALFALFA; Taylor et al. 2012, 2013 in AGES). If some of the HI clouds are probably tidal debris harassed from massive Virgo cluster objects, such as the case of VIRGOHI21 and NGC 4254 (Haynes et al. 2007), others might have been formed from the stripped gas of spirals entering the cluster for the first time (Keent et al. 2009). Interferometric observations have revealed the presence of spectacular tails of HI gas in the Virgo cluster (Oosterloo & van Gorkom 2005; Chung et al. 2007). The typical cometary shape of these features strongly suggests that ram pressure stripping is the responsible process. The main results of these observations are that ram pressure stripping is acting well outside the virial radius of clusters, making this process the most efficient gas stripping process also in regions of relatively low density of the intergalactic medium.

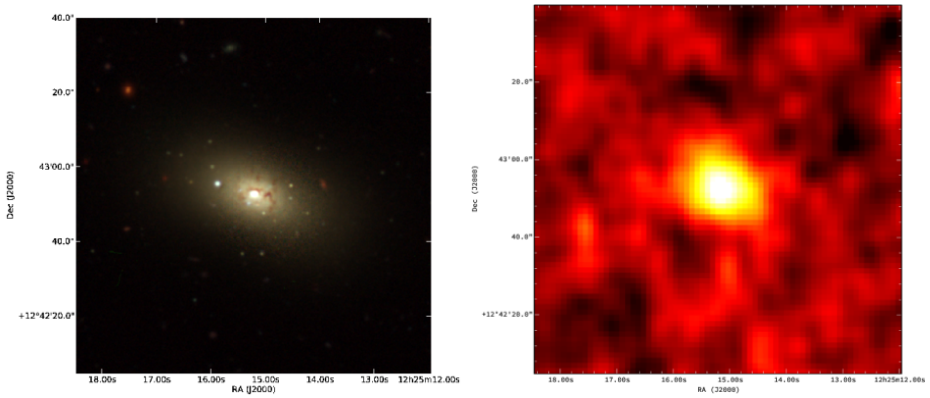

Fig. 10 The NGVS optical color (*top*) and the *WISE* 12 μm (*bottom*) images of the dwarf elliptical VCC 781 in the Virgo cluster. The dust lane present in the optical image is detected in the core of the galaxy in emission in the mid-infrared by *WISE*

The lack of evident associated regions of star formation also indicate that, contrary to what predicted by models (Kepferer et al. 2009), the stripped gas can be hardly transformed into new stars and, eventually, give birth to dwarf galaxies (Boissier et al. 2012; see, however Yagi et al. 2013).

Similar long tails of hot gas have been observed in X-rays with *Chandra* in two spiral galaxies in the cluster A3627 (Sun et al. 2007, 2010). These observations indicate that also the hot halo gas of galaxies can be stripped by ram pressure in high-density environments.

3.3 Dust content

The *Spitzer* and *Herschel* missions allowed a detailed analysis of the mid- and far-infrared properties of local galaxies in high-density environments. The spectral coverage (5–500 μm), combined with the high angular resolution (from a few to 36 arcsec at 500 μm) and the sensitivity of the different instruments were crucial for resolving the different dust components (PAHs, hot and cold dust) in galaxies. The analysis of the brightest Virgo cluster spirals has clearly shown that the cold dust component distributed over the disk is removed with the gaseous component during the interaction with the hot intracluster medium. Indeed, HI-deficient spiral galaxies have truncated dust disks compared to unperturbed field objects (Cortese et al. 2010). Their total dust content is also reduced with respect to normal, field galaxies (Cortese et al. 2012a). Concerning the dwarf galaxy population, de Looze et al. (2010, 2013) have shown the existence of a significant number of dE with presence of dust in their inner regions (Fig. 10). 36 % of the dwarf galaxies belonging to the green valley, identified by Boselli et al. (2008a) as galaxies migrating from the blue cloud to the red sequence (transition type galaxies), have been detected by *Herschel*. There is also evidence of the presence of a residual dust content in several dwarf ETGs located outside the diffuse X-ray emitting gas permeating the cluster (Boselli et al. 2014a). These observations are consistent with the idea that the dust associated with the gaseous phase is removed outside-in during the interaction with the intergalactic medium of galaxies infalling for the first time into the cluster. Their interstellar medium can be retained only in the inner regions, where the gravitational potential well of the galaxy is at its maximum.

3.4 Star formation

The statistical studies of the star-formation properties of cluster galaxies in the past years have been mainly focused on the bright galaxy population. Using a sample of 79 nearby clusters with available multifrequency data, Popesso et al. (2007) have shown that the cluster integrated star-forming properties do not change as a function of the cluster properties. They see, however, that the fraction of blue galaxies depends on the total X-ray luminosity of the clusters, suggesting that environmental processes linked to the presence of the hot X-ray emitting intracluster gas might affect the star-formation history of cluster galaxies. Using a sample of nine nearby clusters, including Coma and A1367, with new spectroscopic data, Rines et al. (2005) have shown that the fraction of star-forming bright galaxies, as determined from the presence of the Balmer Hα emission line, increases with clustercentric distance and reaches that of the field at ~2 to 3 virial radii. This work mainly confirms the first results obtained by Gomez et al. (2003) and Lewis et al. (2002) using the SDSS and 2dF surveys.

The combination of Hα and HI data has been crucial for understanding the very nature of the underlying physical process responsible for the quenching of the star-formation activity of cluster galaxies. This has been possible in the Virgo cluster and in the Coma/A1367 supercluster (Gavazzi et al. 2013a,b). These works have shown that the quenching of the star-formation activity follows the stripping of the atomic gas as indicated by the tight relation between the *SSFR* and the HI-deficiency parameter.[14] Indeed, the specific star-formation rate decreases with the clustercentric distance exactly as the HI-deficiency, making LTGs redder (Gavazzi et al. 2013a,b).[15]

An accurate study of the star-formation properties of low-luminosity cluster galaxies has been made possible owing to the narrow-band Hα imaging data that our team has obtained in these past years. By comparing the Hα morphology of galaxies in Virgo, Coma and A1367 to those of field galaxies selected according to similar criteria, Fossati et al. (2013) have shown that the star-forming disk of LTGs, including dwarf systems, is truncated once the galaxies are devoid of their gas (Fig. 11). The star-formation process is thus quenched outside-in, confirming previous results obtained for the bright galaxy population (Koopmann et al. 2006; Boselli & Gavazzi 2006; Boselli et al. 2006; Cortese et al. 2012b). The Hα imaging of a few dE galaxies have also revealed the presence of an emitting nucleus, suggesting that, after a stripping process, there is still some retention of gas where the gravitational potential well of the galaxy is at its maximum.[16] This gas is able to feed a nuclear star-formation activity (Boselli et al. 2008a). More in general, multizone chemo-spectrophotometric models of galaxy evolution especially tailored to reproduce the effects due to ram pressure stripping in cluster environments have shown that the observed outside-in truncation of the star formation in gas stripped galaxies can be responsible for the inversion of the color gradient observed in massive galaxies (Boselli et al. 2006) or in dwarf ellipticals (Boselli et al. 2008a). There is also evidence of some galaxies with a disturbed

[14] The HI-deficiency parameter is defined as the difference, on logarithmic scale, between the expected and the observed HI gas mass of each single galaxy. The expected atomic gas mass is the mean HI mass of a galaxy of a given optical size and morphological type determined in a complete sample of isolated galaxies taken as reference (Haynes & Giovanelli 1984).

[15] Early claims of enhanced radio-continuum emission from LTGs in the A1367 and Coma clusters (Gavazzi & Jaffe 1985, 1986) are insufficient to infer a significant star-formation enhancement in clusters. It would not be surprising, however, if on a short time scale this would take place from the shocked material during the early phases of a ram pressure event.

[16] Examples of ETGs with nuclear or circumnuclear Hα emission in the Virgo cluster are given in Boselli et al. (2008a): VCC 450, 597, 710, 1175, 1617, 1855, or in Toloba et al. (2014b): VCC 170, 781, 1304, 1684.

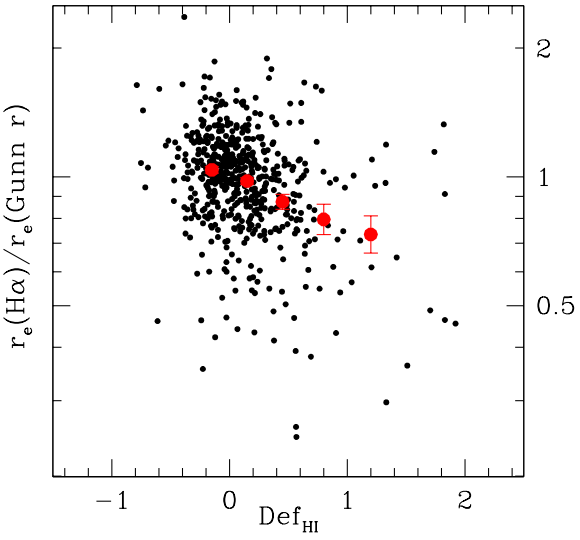

Fig. 11 The relation between the ratio of the Hα (star forming disk) to *r*-band (old stellar population) effective radii and the HI-deficiency parameter. *Big red dots* are average values along the *y*-axis in different bins of HI deficiency, from Fossati et al. (2013). The star-forming disk is truncated once the atomic gas is removed in cluster galaxies. Courtesy of ESO

Hα or UV morphology, witnessing and undergoing interaction with the hostile cluster environment (Smith et al. 2010). The Hα and UV data have been also crucial for studying extraplanar star-formation events in galaxies with clear signs of an undergoing perturbation (see Sects. 3.8 and 4.5).

A systematic study of the star-formation properties of galaxies in 23 nearby ($z \sim 0.06$) groups based on *GALEX* data has been presented in Rasmussen et al. (2012a). This work has shown that, as in clusters, the fraction of star forming galaxies within groups is suppressed with respect to the field in the inner ∼2 virial radii (∼1.5 Mpc). The same work has shown a suppression of the specific star-formation rate by a factor of ∼40 % with respect to the field, quantifying the impact of the group environment on quenching the activity of star formation in infalling galaxies. At fixed galaxy density and stellar mass, this suppression is stronger in more massive groups. Rasmussen et al. (2012a) concluded that the average time scale for quenching the star-formation activity is $\gtrsim$2 Gyr and identified a combination of tidal encounters and starvation as the responsible process.

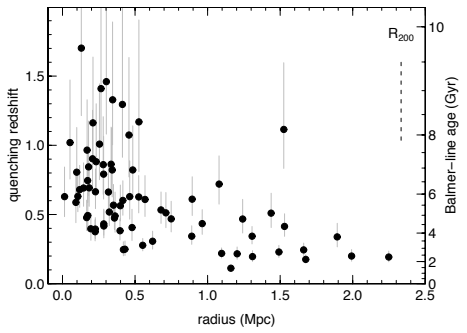

Fig. 12 The dependence of the quenching age, defined as the redshift for which the look-back time is equal to the age of dwarf galaxies determined using the Balmer lines, on the projected distance from the core of the Coma cluster, from Smith et al. (2008). Dwarf elliptical galaxies in the periphery of the Coma cluster stopped their activity of star formation only at recent epochs. Reproduced with permission of Oxford University Press

3.5 Stellar populations

The study of the nature of the various stellar populations of dwarf galaxies in different environments is one of the topics that has improved the most in the past years owing to the advent of large photometric and spectroscopic surveys of nearby clusters. The most recent works have been mainly focused either on the optical (Haines et al. 2006b; Lisker et al. 2006a, 2008; Misgeld et al. 2009; Janz & Lisker 2009; Gavazzi et al. 2010; Scott et al. 2013; den Brok et al. 2011; McDonald et al. 2011) or on the optical-UV CMR (Boselli et al. 2005a,b, 2008a, 2014a; Lisker & Han 2008; Haines et al. 2008; Kim et al. 2010; Smith et al. 2012b), or based on the analysis of absorption line indices obtained from deep spectroscopic observations (Smith et al. 2006, 2008, 2009, 2012a; Haines et al. 2006, 2007; Michielsen et al. 2008; Toloba et al. 2009; Paudel et al. 2010a,b, 2011; Boselli et al. 2014a). The first works of Haines et al. (2006a,b) on the cluster A2199 and on the Shapley supercluster, along with that of Smith et al. (2006) on 94 clusters with spectroscopic data from the SDSS, have consistently shown a different evolution of massive and dwarf galaxies in high-density regions. While the fraction of massive ($M_r < -20$) red galaxies dominated by an old population gradually decreases from ∼80 % in the core to ∼40 % in the periphery (3–4 virial radii) of the cluster, the radial variation for dwarfs ($-19 < M_r < 17.8$ mag) is much more pronounced, from ∼90 % in the core to ∼20 % at one virial radius (Haines et al. 2006a,b; Boselli et al. 2014a). Consistently, by studying the dispersion of the fundamental

plane relation of early-type systems, Smith et al. (2006) have shown that, for a given velocity dispersion—thus total mass—galaxies in the periphery of clusters have stronger Balmer absorption lines, indicative of younger ages than those located in the cluster core (see Fig. 12). Consistent results have been obtained using new spectroscopic observations in the Coma cluster by Smith et al. (2008, 2009, 2012a). All these studies have indicated strong Balmer absorption lines and enhanced α/Fe ratios in the red dwarf galaxy population in the outskirts of Coma compared to the core, where only the oldest galaxies reside, consistent with a relatively recent formation of the red sequence ($0.4 < z < 0.7$). The SW substructure of Coma is also composed of younger dwarf quiescent galaxies, probably formed between $0.1 < z < 0.2$ (Smith et al. 2009). The mean age of the underlying stellar population is mainly related to the total mass of galaxies in massive objects ($M_{\rm star} > 10^{10}$ M$_\odot$) and only marginally on the environment, while the reverse holds for dwarf systems. Indeed, the mean age of the stellar population of dE galaxies is about a factor of two younger at one virial radius than in the core of the cluster (Smith et al. 2012a). The earlier work of Poggianti et al. (2004) has shown the presence of low luminosity post-starburst galaxies in the Coma cluster, consistently with the picture where dwarf galaxies abruptly truncated their star-formation activity and became red objects. These post-starburst galaxies are mainly low mass systems situated around massive clusters, as indicated by the recent spectroscopic survey of 48 nearby clusters ($0.04 < z < 0.07$) of Fritz et al. (2014). Similar trends between the mean age of the stellar populations and the clustercentric distance have been also observed in the Virgo cluster by Michielsen et al. (2008), Toloba et al. (2009, 2014b), and Paudel et al. (2010a, 2011). In particular, Toloba et al. (2009) have shown that dE galaxies characterized by the youngest stellar population not only are located in the periphery of the cluster, but also are generally rotationally supported systems. Thanks to the proximity of the Virgo cluster, spectroscopic studies have been used to investigate stellar population gradients within the disk of dwarf elliptical galaxies. The available works have consistently shown that, on average, the mean age of the stellar populations increases from the center to the outskirts of galaxies (Chilingarian et al. 2009; Koleva et al. 2009, 2011; Paudel et al. 2011) contrary to what generally happens in massive systems (Fig. 13). All these evidences are consistent with a scenario where low-luminosity star-forming galaxies recently entered the cluster environment, losing their gas content and quenching their star-formation activity, thus becoming dwarf ellipticals (Boselli et al. 2008a; Toloba et al. 2009; Gavazzi et al. 2010; Koleva et al. 2013).

The study of the photometric properties of cluster galaxies has been primarily aimed at understanding whether genuine giant ellipticals and dwarf systems follow the same CMR, an indication that would suggest a common origin for the two families of objects. The works done so far do not bring fully consistent results. A unique CMR has been invoked by Misgeld et al. (2009) in the Centaurus cluster, by Hammer et al. (2010b) in Coma and more recently by Smith Castelli et al. (2013) by combining SDSS data of Virgo galaxies with those obtained by the ACS Virgo Cluster Survey. Conversely, variations of the CMR have been found using SDSS data of more than 400 Virgo objects by Janz & Lisker(2009). These authors, however, concluded that this observational result does not rule out a common origin for the two populations. Lisker et al. (2008) looked for any systematic difference in the optical CMR of the different subclasses of dwarf elliptical galaxies. Their analysis has shown that, at relatively high luminosities, nucleated dwarf ellipticals have redder colors than normal dE, while the variations with local galaxy density, if present, are minor.

The works of Haines et al. (2008) and of Gavazzi et al. (2010) have been fundamental to extend these interesting results to other environments such as the periphery or rich clusters or intermediate mass groups. Using the $NUV - i$ color index, much more sensitive to age variations than the optical colors, Haines et al. (2008) have shown that the red sequence is not

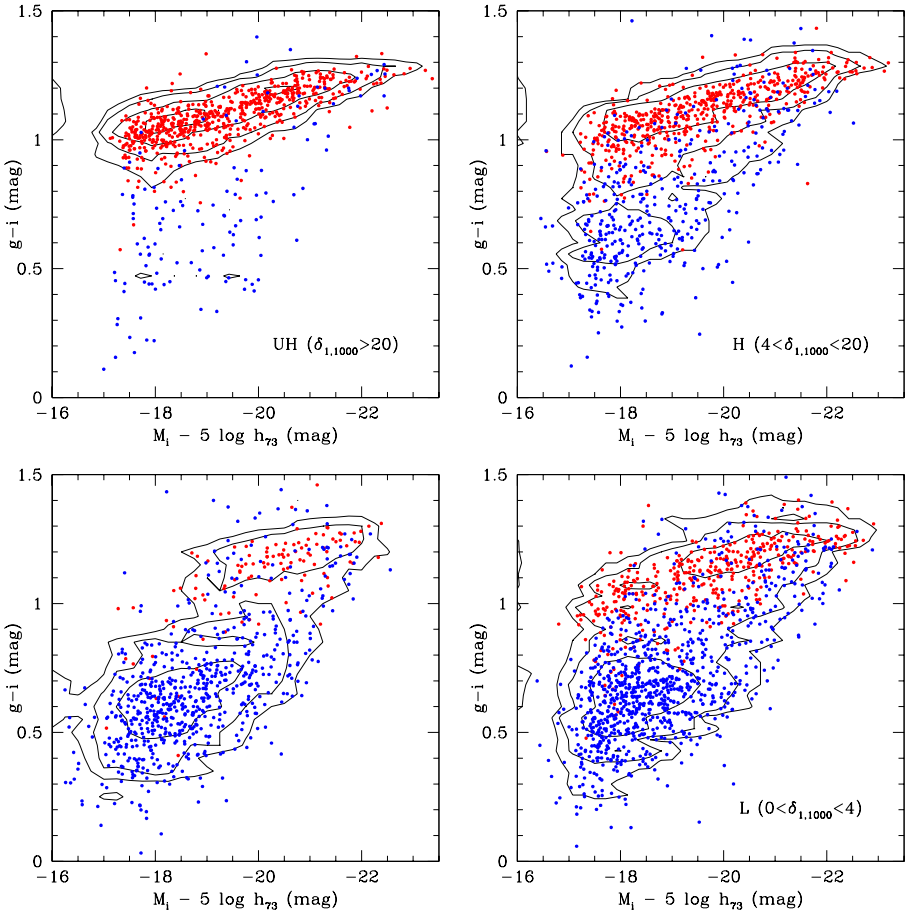

Fig. 13 The $g - i$ vs. M_i CMR for galaxies in the Coma/A1367 supercluster from very high density regions in the core of Coma and A1367 to very low density regions in the voids surrounding the clusters, clockwise from upper left. *Red symbols* indicate early-type galaxies in the red sequence, *blue symbols* late-type systems in the blue cloud, from Gavazzi et al. (2010). Star forming systems are virtually lacking in the densest regions in the core of the clusters, while the faint end of the red sequence is not present only in the lowest density regions dominated by star forming systems. Courtesy of ESO

formed in the field at low luminosities. The faint end of the red sequence, however, is already formed within the different substructures of the Virgo cluster characterized by a wide range in galaxy density (Boselli et al. 2014a). Consistently, Gavazzi et al. (2010) have shown that both the shape of the luminosity function determined for galaxies selected according to their color, and the $g-i$ CMR change as a function of galaxy density, indicating that the processes that gave birth to the faint end of the red sequence have been efficient also in relatively low-density environments. These results are fully consistent with those determined by analyzing statistically significant samples extracted from the SDSS indicating that red dwarf galaxies are extremely rare in the field (Geha et al. 2012). The work of Gavazzi et al. (2010) have also revealed the presence of low-luminosity galaxies with clear signs of a recent activity of

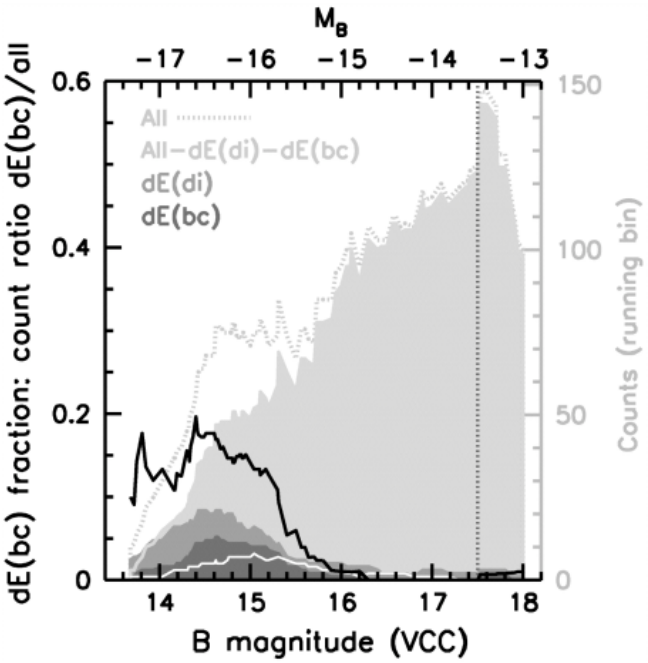

Fig. 14 Histogram of the number of dwarf elliptical galaxies in the Virgo cluster in bins of absolute B band magnitude (from the VCC; right y-axis). The *light gray dashed line* shows the distribution of all dEs, the dark gray area that of dEs with blue nuclei, the medium grey that of dEs with an underlying disky structure, the light gray that of all dEs galaxies after excluding those with disky structures and blue nuclei. The *black solid line* shows the fraction of the dEs with blue nuclei (left y-axis), from Lisker et al. (2006b). © AAS. Reproduced with permission

star formation (post-starburst) in Coma and A1367. These galaxies are analogous to those found in the Virgo cluster by Boselli et al. (2008a) and originally defined as transition type galaxies as their spectrophotometric properties indicate a recent abrupt truncation of their star-formation activity (Koleva et al. 2013).

The works of van den Bosch et al. (2008), Wilman et al. (2010), and Cibinel et al. (2013) studied the relationship between galaxy color and density in nearby groups using SDSS photometric data. These works have shown that the perturbation induced by the environment affects more the color than the morphology of galaxies (van den Bosch et al. 2008). They have also shown that galaxies become red only once they have been accreted on to halos of a certain mass (Wilman et al. 2010). The quenching of the star-formation activity is primarily in the outer disk of galaxies entering groups (Cibinel et al. 2013).

3.6 Structural parameters

The study of the structural properties of dwarf galaxies in nearby clusters has enormously benefited from the SDSS. The first systematic study of the structural properties of dwarf elliptical and spheroidal galaxies in the Virgo cluster has been done by Lisker and collaborators (Lisker et al. 2006a,b, 2007, 2009; Janz & Lisker 2008; Lisker 2009). These works basically extended previous analyses done on the photographic plates taken at the Du Pont

telescope at Las Campanas in the eighties by Binggeli and collaborators (Binggeli et al. 1985; Binggeli & Cameron 1991). Lisker et al. (2006a) have looked for unseen disky features such as spiral arms, bars, and edge-on disks in dwarf ellipticals by applying unsharp masks or subtracting the axisymmetric light distribution of each galaxy from the image in a complete sample of Virgo galaxies extracted from the SDSS. They have shown that dE galaxies with typical spiral features, as the one first discovered by Jerjen et al. (2000), are rather common objects. Among the brightest dwarf ellipticals, ∼50 % of the objects possess these features, while their fraction decreases with decreasing luminosity (Fig. 14). Such galaxies have been later discovered in other clusters like Coma using the exquisite quality images obtained with the HST (Graham et al. 2003; den Brok et al. 2011; Marinova et al. 2012). Their spiral structure is generally grand design and not flocculent, and they have a flat shape suggesting that they are genuine disk galaxies (Lisker et al. 2006a; Lisker & Fuchs 2009). The best quality imaging material gathered thanks to the ACSVCS survey of Virgo has shown that these kind of features are very frequent in quiescent systems of intermediate luminosity (Ferrarese et al. 2006). The same survey has also indicated that dusty features observed in absorption are also quite frequent but mainly in the most massive objects (42 %). There is also a population of dwarf ellipticals with blue nuclei probably due to a recent episode of star formation. The work of Lisker et al. (2007) has shown that galaxies with disky structures, including those with blue nuclei, are not distributed near the cluster core as are the bright ellipticals and lenticulars, or the other ordinary spheroidal dwarf ellipticals, but are rather distributed uniformly all over the cluster. Thanks to HST images it has also been shown that dwarf ETGs in the periphery of the Peresus cluster have more disturbed morphologies than those located in the core of the cluster (Penny et al. 2011). Lisker et al. (2009) have studied the properties of the nucleated dwarf elliptical galaxies without any sign of recent star formation (blue nuclei) or disky structure (spiral arms, bars, disks) located close to the bright central elliptical galaxies. By dividing the sample into fast- and slow-moving objects according to their velocity with respect to the mean recessional velocity of the cluster, they have shown that fast-moving objects have a projected axial ratio consistent with a flatter shape, while the slow-moving are roundish objects. Deep near-infrared images of dwarf elliptical galaxies have also revealed different structures in their 2D-stellar distribution (Janz et al. 2012, 2014). All these results have been interpreted as an evidence that dwarf elliptical galaxies have different origins. Those presenting disky structures, or having a flat shape (thus having a high-velocity with respect to the cluster) have been recently accreted as star-forming systems and have been transformed during their interaction with the cluster environment, while the roundish objects with a low-velocity dispersion have been in the cluster since a very early epoch, or might have even been formed within the cluster.

In the recent years a huge effort has also been made at understanding whether dwarf elliptical galaxies are just the low luminosity extension of bright ellipticals or rather are a totally independent category of objects. Systematic differences in the two galaxy populations, and possible similarities with the properties observed in spiral galaxies, could be interpreted as a clear indication of a different formation scenario (Kormendy et al. 2009; Kormendy & Bender 2012). The debate is principally motivated by the possible existence of a few dwarf elliptical galaxies similar to M32 that, contrary to the general dE galaxy population, have a very compact structure characterized by a very high surface brightness. These objects might not follow the standard scaling relations depicted by the other quiescent systems. The seminal work of Graham & Guzman (2003) has clearly shown that the observed change in slope in the surface brightness vs. absolute magnitude relation observed between massive and dwarf ellipticals is naturally due to the shape of their Sersic light profile, with an index n increasing with the luminosity. Continuity between E and dE in different scaling relations

has been also reported by Gavazzi et al. (2005), Ferrarese et al. (2006), Misgeld et al. (2008, 2009), Misgeld & Hilker (2011), and Smith Castelli et al. (2013). On the contrary, there is evidence that the size–luminosity relation depicted by bright ellipticals is not followed by dwarf systems, that rather have an almost constant extension ($R_{\rm eff} \simeq 1$ kpc) regardless of their luminosity (Janz & Lisker 2009; Smith Castelli et al. 2008; Misgeld & Hilker 2011). This dispute will certainly come to an end once the NGVS survey (Ferrarese et al. 2012), that has covered homogeneously the whole Virgo cluster, thus including several hundreds of early-type systems in four (u^*, g', i', z') photometric bands, will be fully exploited.

Thanks to its exquisite angular resolution, the ACSVCS (Cote et al. 2004) allowed the detailed analysis of the structural properties of the nuclei of ETG. The HST data have shown that ground based optical surveys generally underestimate the presence of nuclei in ETGs probably because of their limited angular resolution (Cote et al. 2006). The nuclei are generally resolved even in dwarf systems, ruling out any possible low-level AGN nature (Cote et al. 2006). The same data have also shown the lack of any strong evidence that nucleated galaxies are more centrally clustered than other non-nucleated objects. By fitting their radial light distribution, Cote et al. (2007) have shown that a Sersic profile generally overestimates the nuclear emission in bright and massive galaxies while it underestimates it in low-luminosity objects, with a difference that steadily varies with galaxy luminosity. They discussed the observed nuclear properties of ETGs in the context of gas infall in various formation scenarii.

The comparison of the structural properties of red sequence and blue cloud galaxies in nearby groups has been carried out by van den Bosch et al. (2008) using a large sample of galaxy groups extracted from the SDSS. Studying their color and light concentration, their analysis has shown that the transformation mechanism operating on satellites affects more colors than morphology. They have also shown that the observed differences between satellite and central galaxies do not depend on the halo mass, suggesting that the process at the origin of the observed perturbation is the same in different environments. They thus concluded that the most probable process is starvation since they considered ram pressure stripping and galaxy harassment efficient only in high-mass systems such as clusters.

3.7 Kinematics

The kinematical properties of galaxies and their relations with the environment have been the subject of various works done by the SAURON (Bacon et al. 2001), ATLAS^{3D} (Cappellari et al. 2011a), CALIFA (Sanchez et al. 2012) and SMAKCED (Toloba et al. 2014a) teams. While the first three projects were mainly focused on bright galaxies (see, however, Rys et al. 2013), with SAURON and ATLAS^{3D} primarily on early-type systems, SMAKCED was devoted to the study of dwarf elliptical galaxies in the Virgo cluster. The final purpose of this project was that of understanding whether dE are rotationally supported systems, as first claimed by Pedraz et al. (2002), Geha et al. (2002, 2003) and van Zee et al. (2004). Based on very small samples, these pioneering works were mainly limited by the spectral resolution of the adopted instruments, barely sufficient to observe velocity dispersions of the order of 20–30 km s^{-1} typical of dwarf systems. Using a sample of 21 dwarf elliptical galaxies mainly located in the Virgo cluster, Toloba et al. (2009, 2011) have shown the existence of a large fraction of rotationally supported dE. Their analysis indicated that pressure-supported systems, generally characterized by old stellar populations, are located preferentially in the inner regions of the cluster, while rotationally supported objects, composed of younger stellar populations, are mainly located at the periphery of the cluster (Toloba et al. 2009). Further-

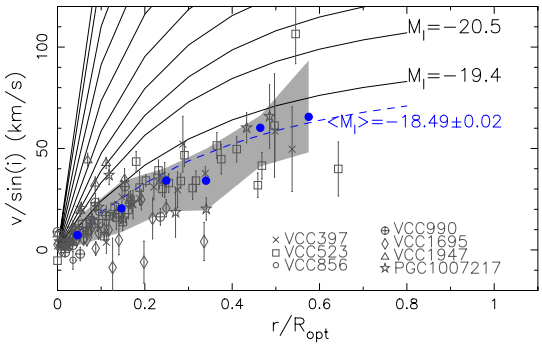

Fig. 15 The observed rotation curves of rotationally supported systems dEs (*gray symbols*) are compared to the mean rotation curves of observed (*black solid lines*) and expected (*blue dashed line*) late-type galaxies of different absolute *i*-band magnitude. *Blue filled dots* represent the median observed rotation curve of rotationally supported dEs, while the gray area the rotation velocities within 1 σ from the median, from Toloba et al. (2011). The rotation curves of rotationally supported dEs are similar to those of star forming systems of comparable luminosity. Courtesy of ESO

more, these works have shown that rotationally supported dE have rotation curves similar to those of LTGs of similar luminosity and follow the same Tully–Fisher relation as star forming systems (Toloba et al. 2011; Fig. 15). The analysis of the main scaling relations, such as the Faber–Jackson and the Fundamental Plane relations, consistently revealed that dE are different from massive ellipticals since have structural and kinematical properties closer to those of star-forming systems rather than to those of E and S0 (Toloba et al. 2012). Although the kinematical properties of dE might change from object to object (Rys et al. 2013), all these observational evidences are consistent with the picture where gas-rich star-forming systems entering the hostile cluster environment lose their gaseous component on relatively short time scales, stopping their activity of star formation and becoming quiescent systems. The angular momentum of the galaxy is conserved on relatively long time scales if the galaxy interacts with the hot intergalactic medium (ram pressure stripping), while the system is heated if the dominant process is gravitational (galaxy harassment). The observations indicate that the dynamical interactions with the IGM are dominant at the present epoch, producing the rotationally supported systems at the periphery of the cluster, while the gravitational one, dominant in the past, produced the hot systems mainly located in the virialized inner region of the cluster (Toloba et al. 2014b; Boselli et al. 2014a). Independent evidence of gravitational interactions comes also from the presence of dE with counter rotating cores observed by Toloba et al. (2014c) close to the Virgo cluster core. This evolutionary picture is consistent with that proposed for more massive galaxies by the ATLAS^{3D} survey, where the most massive slow rotators are formed by major dry merging events, while fast rotators by the quenching of the star formation of spiral galaxies (Cappellari et al. 2011b; Cappellari 2013). The only difference with the fading model proposed for low luminosity systems is that, associated with the quenching of the star-formation activity of spiral disks in cluster, there is also a growth of the bulge (Cappellari 2013).

3.8 Individual galaxies

As already introduced in Sect. 1, a typical example of galaxies undergoing environmental transformations is the galaxy FGC 1287 at the periphery of the cluster Abell 1367, showing a cometary HI tail of 250 kpc projected length. Although the origin of this feature is still uncertain (Scott et al. 2012), its typical shape suggests that it might have been created by the interaction of its ISM with the hot and dense ICM of the cluster during a ram pressure stripping event. We recall that this result agrees with the presence of massive ram pressure stripped galaxies up to more than 1 Mpc away from the cluster core observed in several nearby clusters as summarized in Boselli & Gavazzi (2006), including a recent discovery in the Shapley supercluster (Merluzzi et al. 2013). It also agrees with the results of the most recent hydrodynamical simulations of gas stripping in cluster galaxies (see Sect. 4.2).

Consistent with this scenario is also the discovery of cluster galaxies with long tails of ionized gas, first observed in A1367 by Gavazzi et al. (2001) and later in Virgo (Yoshida et al. 2004; Kenney et al. 2008), in Coma (Yagi et al. 2007, 2010; Yoshida et al. 2008, 2012; Fossati et al. 2012), and in A3627 (Zhang et al. 2013). If the Hα filamentary structure associated with NGC 4388 in Virgo is located close to the cluster core (Yoshida et al. 2004; kenney et al. 2008), those relative to the galaxies in A1367 and Coma are much more in the periphery of the clusters, again indicating that ram pressure stripping is efficient not only in the cluster core. The observation of these peculiar objects gives also other important information on the physical process acting on cluster galaxies. They first indicate that the stripping process is also able to remove the ionized phase of the gas (Gavazzi et al. 2001). There are, however, other indications that part of the gas can be ionized in situ by shocks (Yoshida et al. 2012). They indicate that star formation in the stripped gas, if present, is generally very modest and located in small (~200 to 300 pc) defined knots of stellar mass 10^6–10^7 $M_\odot$ (Yoshida et al. 2008). The few star-forming blobs associated with NGC 4388 or with the interacting systems VCC 1249–M49 in Virgo are even smaller, with stellar masses $\lesssim 10^{4.5}$ $M_\odot$ (Arrigoni Battaia et al. 2012; Yagi et al. 2013). This result is consistent with the evidence that the efficiency of star formation in the stripped material is lower than the standard efficiency observed over spiral disks generally described by the Schmidt law (Boissier et al. 2012).

This last result is of particular importance in constraining models of star formation from the stripped gas (see Sect. 4.5). Indeed, it indicates that the formation of dwarf galaxies in the stripped material, if possible, is not frequent and cannot produce any significant steepening of the faint end of the luminosity function. There are, however, a few cases where the star-formation process in the stripped gas is important. First discovered by Cortese et al. (2007) in two clusters at $z \sim 0.2$, there exist a few objects with long tails of star-forming regions prominent in UV images generally named "fireballs" or "jellyfish" (Smith et al. 2010). They are more frequent in massive clusters such as Coma than in small systems as Virgo. An exception to this rule is the spectacular IC 3418 (VCC 1217) close to the core of the Virgo cluster (Hester et al. 2010; Fumagalli et al. 2011; Jachym et al. 2013; Kenney et al. 2014). The galaxy, totally stripped of its gas, quenched its activity of star formation ~300 to 400 Myr ago probably after a starburst activity. In the tail, the observed Hα peaks are displaced from the UV emitting knots, suggesting that the gas clumps are continuously accelerated by ram pressure, leaving behind new stars decoupled from the gas (Kenney et al. 2014). The typical mass of these fireballs is of ~10^5 $M_\odot$ (Fumagalli et al. 2011), thus still too small to make this process relevant for the formation of dwarf galaxies or for modifying the shape of the luminosity function. Another spectacular example with similar characteris-

tics is the galaxy ESO 137-001 in the Norma cluster (A3627, Sun et al. 2007; Jachym et al. 2014).

Multifrequency observations have been critical to demonstrate that also the hot X-ray emitting gas in the halo of galaxies can be stripped by ram pressure in cluster (Sun et al. 2007, 2010; Ehlert et al. 2013; Zhang et al. 2013) and group galaxies (Rasmussen et al. 2012b). The most evident case is the galaxy ESO 137-001 in A3627 (Sun et al. 2007; Fumagalli et al. 2014). While in clusters the hot and cold gas removal is primarily due to ram pressure stripping, in groups both ram pressure and tidal interactions contribute, as clearly indicated by the recent *Chandra* and VLA observations of the nearby group of NGC 2563 (Rasmussen et al. 2012b). The importance of these results resides in the fact that they are the first observational justification that the gaseous halo of galaxies is removed in high-density environments, as generally assumed in cosmological and semi-analytic models of galaxy evolution. This assumption in models and simulations is crucial since it makes the feedback process of supernovae extremely efficient in expelling the disk gas, thus quenching the activity of star formation and transforming on very short time scales gas-rich systems into quiescent, red galaxies (see Sect. 4.1).

Although not frequent because of the high-velocity dispersion within clusters, tidal interactions can also be related to the formation and evolution of dwarf systems in high-density regions. There exists, indeed, a few representative and interesting cases in nearby clusters. One example is NGC 4254 in Virgo. Entering the cluster at high velocity for the first time, the galaxy was harassed of a fraction of its gas that is now forming a cloud (VIRGOHI21; Davies et al. 2004) apparently not associated with any other optical counterpart (Haynes et al. 2007; Duc & Burnaud 2008; Wezgowiec et al. 2012). The wide field and the high sensitivity to low surface brightness features of the NGVS survey allowed the identification of three dwarfs galaxies satellite of the bright NGC 4216 in Virgo undergoing a tidal disruption process (Paudel et al. 2013). The data obtained by NGVS and GUViCS have shown the presence of small star-forming complexes produced during the interaction of the dwarf, gas-rich Im galaxy VCC 1249 (UGC 7636) with the bright elliptical M49 (Arrigoni Battaia et al. 2012). Although the stellar mass of these objects is still very small ($10^4 - 10^5\,M_\odot$), it has been suggested that a similar process might have been at the origin of Ultra Compact Dwarf (UCD) galaxies, a population recently discovered in high-density regions (Drinkwater et al. 2004). We can also mention the discovery of a blue infalling group in A1367, the prototypal example of pre-processing in the nearby universe (Sakai et al. 2002; Gavazzi et al. 2003b; Cortese et al. 2006b). The low-velocity dispersion within a group infalling into the main cluster makes gravitational interactions very efficient in perturbing galaxies before they become real members of A1367. These perturbations produce small condensations of matter that might later evolve as independent entities and thus be progenitors of dwarf cluster galaxies.

4 Modeling

4.1 Cosmological simulations

Cosmological models of galaxy evolution indicate that galaxies are formed from the condensation of gas within dark matter halos. In a hierarchical formation scenario, small structures are formed first and later merged to give birth to massive objects. By cooling, the gas conserves its angular momentum leading to the formation of rotating systems. The violent interactions associated with merging events heat the systems, forming bulges and ellipticals. In

this bottom-up formation scenario, galaxies now belonging to rich clusters might have suffered the effects of different environments during their life (pre-processing; Dressler 2004). They might have been members of small groups where gravitational interactions with other members were important before entering the evolved cluster (Boselli & Gavazzi 2006).

As described in De Lucia (2011), in cosmological simulations the physical evolution of galaxies is reproduced using various techniques. Hydrodynamical simulations mimic the evolution of the gaseous component modeling different physical processes such as gas cooling, star formation, and feedback. Because of this complex approach, these simulations are limited by spatial and mass resolution (e.g. Berlind et al. 2005). In semi-analytic models of galaxy formation (SAM), the link between the evolution of dark matter halos traced by high-resolution N-body simulations and the barionic matter is accomplished using simple physical prescriptions, without following explicitly the coupled evolution between structure formation and gas physics through the numerical integration of hydro/gravity equations. Nevertheless this (computationally cheap) approach has the advantage of covering a significantly larger range in stellar mass and spatial resolution and thus is well suited for the study of the evolution of dwarf systems in different environments as those analyzed in this work.

Beside "harassment" (Moore et al. 1996), other investigations of the effects of the cluster environment in cosmological hydrodynamical simulations have been undertaken by McCarthy et al. (2008). In this work the authors simulated the stripping[17] of the hot halo of satellite galaxies entering massive halos typical of groups and clusters. These simulations indicated that an important fraction of the hot gas of satellite galaxies ($\sim$30 %) is still at place 10 Gyr after the beginning of the interaction. More recently, Bahe et al. (2012) and Wetzel et al. (2013) concluded that the confinement pressure exerted by the intracluster medium is not sufficient to significantly decrease the impact of the ram pressure exerted on the hot gas halo of satellite galaxies. Using the same cosmological simulations, the same team has also shown that ram pressure stripping exerted by the extended gas halo surrounding groups and clusters is sufficiently strong to strip the hot gas atmosphere of infalling galaxies up to $\sim$5 times the virial radius (Bahe et al. 2013). These results are consistent with the simulations of Cen et al. (2014).

The most recent semi-analytic models of galaxy evolution arrive to reproduce massive and dwarf galaxies down to stellar masses of $\sim 10^{7.5}$ (Guo et al. 2011, 2013) and sample a large range in environments, from the field to massive clusters analog to Coma in the local universe (some 10^{15} $M_{\odot}$). Only some of the most recent models, however, have implemented tuned recipes such as those proposed by McCarthy et al. (2008) to accurately reproduce the effects induced by the group and cluster environment on galaxy evolution (Font et al. 2008; Kang & van den Bosch 2008; Kimm et al. 2009; Taranu et al. 2014; Weinmann et al. 2011; Lisker et al. 2013, the last two especially tailored to mimic the dwarf galaxy populations in local clusters such as Virgo and Coma). Indeed, in previous studies the effects of the environments were simulated just by instantaneously removing the whole hot-gas halo of galaxies once they became satellites. This assumption makes supernova feedback sufficient to totally sweep the cold gas disk that, in the lack of a surrounding halo, is permanently ejected in the

[17] There is a clear inconsistency in the definition of ram pressure and starvation in cosmological simulations and semi-analytic models with respect to the observation and the simulations of single galaxies in local clusters. Cosmologists indistinctly define ram pressure, starvation or strangulation the removal of the hot gaseous halo of satellite galaxies entering the extended gas halo surrounding groups and clusters. In the study of nearby objects, ram pressure stripping is generally referred to the stripping of the cold gas component exerted by the hot cluster intergalactic medium on galaxies moving at high velocity. In the same studies, starvation or strangulation refers to the gas consumption via star formation of galaxies once the infall of pristine cold gas is stopped.

intracluster medium. The lack of gas quenches the activity of star formation on very short time scales producing a large fraction of red galaxies (Kang & van den Bosch 2008; Font et al. 2008; Kimm et al. 2009; De Lucia 2011). For this reason Okamoto & Nagashima (2003) and Lanzoni et al. (2005) identified starvation as the main physical process responsible for the quenching of the star-formation activity of cluster galaxies.

Despite the implementation of tuned recipes for mimicking the stripping of the hot gas, the results of the most recent semi-analytic models still overpredict the number and the colors of red objects (Fontanot et al. 2009; Wang et al. 2012), suggesting that the effects induced by the environments are overestimated (Weinmann et al. 2011; Fig. 16).

The same models, based on the MS-II simulations of Guo et al. (2011) including a physical prescription for the stripping of the hot gas and supernova feedback, reproduce well the velocity dispersion and the luminosity functions of nearby clusters, but overpredict the dwarf to giant fraction probably because of an incorrect prescription for tidal disruption (see however Henriques et al. 2013).

Several works have also indicated that the evolution of cluster galaxies might have been affected during their previous membership to groups (pre-processing) (Book & Benson 2010; De Lucia et al. 2012; Bahe et al. 2013; Lisker et al. 2013; Taranu et al. 2014). For this reason, gas stripping and quenching of the star formation might have happened at earlier epochs and outside the virial radius of the evolved cluster (Bahe et al. 2013). The models also indicate that pre-processing might have been more important in low-mass systems than in massive galaxies (De Lucia et al. 2012). Models thus suggest that dwarf elliptical galaxies in local clusters might have been processed early and continuously in groups and cluster halos instead of being late-type objects recently transformed in quiescent systems (Lisker et al. 2013; Taranu et al. 2014).

4.2 Hydrodynamical simulations of gas stripping

Different teams developed their own hydrodynamical simulations to reproduce the effects induced by the hostile cluster or group environment on galaxy evolution. Tonnesen et al. (2007) tried to identify, using cosmological simulations, which, among the different processes acting on galaxies in rich cluster, is the dominant one. Their work has indicated that the interaction with the hot intergalactic medium (ram pressure stripping) is the most important at the present epoch. Models and simulations indeed show that, although dominant in the core of the cluster where the velocity of the galaxy and the density of the ICM are maximal, ram pressure stripping is an ongoing process eroding the gaseous component all over the orbit of the galaxy within the cluster (Roediger & Hensler 2005; Roediger & Bruggen 2006, 2007; Bruggen & De Lucia 2008; Kapferer et al. 2008). The simulations of Tonnesen et al. (2007) indeed indicate that ram pressure is an important process out to the virial radius, able to remove all the gas on time scales of the order of $\geq$1 Gyr. The limit on the cluster region where ram pressure stripping is active and efficient has been later extended to $\sim$3 virial radii by Cen et al. (2014), consistent with the most recent observations of head-tail galaxies in the periphery of nearby clusters (see Sect. 3.8). Timescales of the order of 1.5 Gyr are also obtained using 3D hydrodynamical simulations by Roediger & Bruggen (2007) and Cen et al. (2014) for a substantial reduction of the total gas content of the perturbed galaxy via ram pressure. As mentioned before, however, these hydrodynamical simulations based on a single and homogeneous gas phase for the ISM generally underestimate the efficiency of ram pressure stripping (Tonnesen & Bryan 2009). Multiphase hydrodynamical simulations indicate that gas ablation in all its phases (from diffuse atomic to dense molecular gas) can

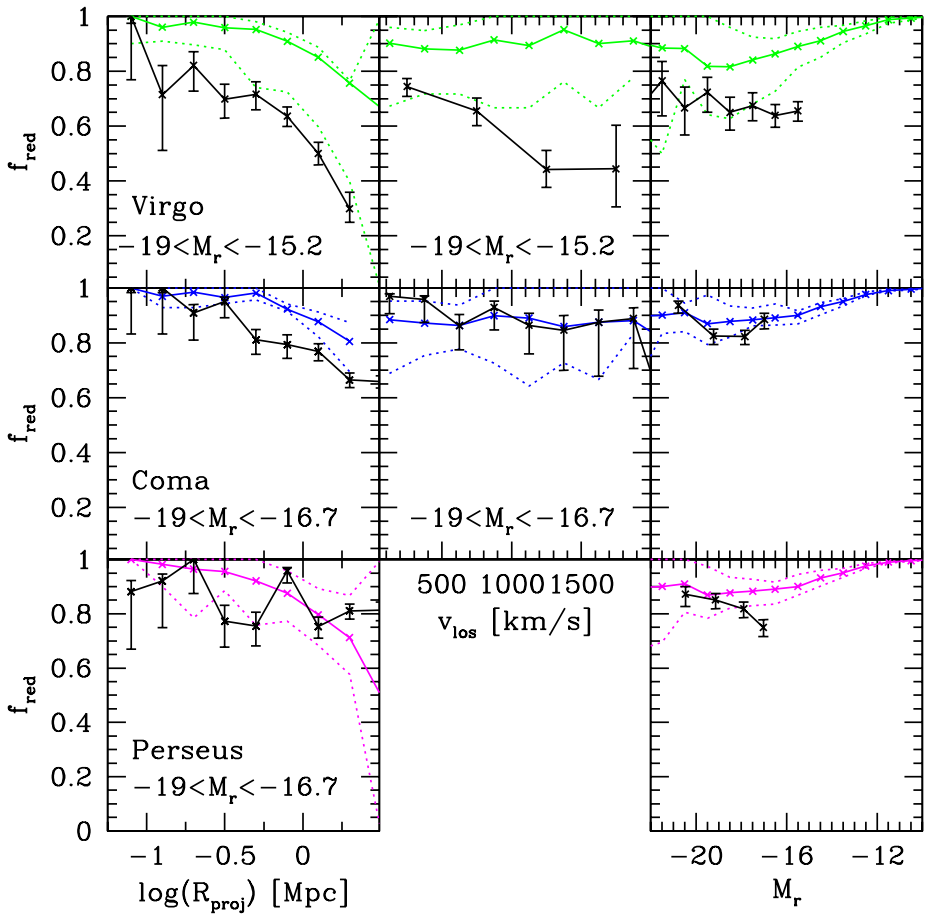

Fig. 16 Fraction of red galaxies as a function of the projected distance from the cluster center (*left panels*), line-of-sight velocity with respect to the cluster center (*central panels*), and absolute magnitude (*right panels*), from Weinmann et al. (2011). Observations of the Virgo cluster (*first row*), of the Coma cluster (*central row*), and of the Perseus cluster (*lower row*) are shown with *black lines* and *relative errorbars*, while the results of the semi-analytic models are the colored lines. The semi-analytic models of galaxy evolution overpredict the number of red, quiescent galaxies especially at low stellar masses or in clusters still under formation (Virgo). This suggests that the gas stripping process and the subsequent quenching of the star formation activity as predicted by models, which happens mainly in groups during the pre-processing of galaxies, is too rapid (Weinmann et al. 2011). Reproduced with permission of Oxford University Press

take place at all galactic radii if ram pressure stripping is sufficiently strong, as it is the case in rich clusters of galaxies such as Virgo (Tonnesen & Bryan 2009) and as seen in the few extreme cases of ram-pressure known to date. Modeling the effects of ram pressure on a multiphase gas disk is still challenging since it requires to take into account several physical effects as to resolve hydrodynamic and thermal instabilities across a large range of physical scales, such as heating and cooling of the ISM, self-gravity, star formation, stellar feedback, and magnetic field. Given the fractal distribution of the gaseous component within the ISM, models must also predict simultaneously the gas distribution on different scales, from giant molecular clouds to the tails whose size can exceed the size of galaxies (Roediger 2009).

Tonnesen & Bryan (2009) performed high-resolution (40 pc) 3D hydrodynamical simulations of galaxies undergoing a ram pressure stripping event. They have included in their code radiative cooling on a multiphase medium. This naturally produces a clumpy ISM with densities spanning six orders of magnitude, thus quite representative of the physical conditions encountered in normal, LTGs. Their simulations show that under these conditions the gas is stripped more efficiently up to the inner regions with respect to an homogeneous gas. They also show that all the low-density, diffuse gas is quickly stripped at all radii. When the ram pressure stripping is strong there is also less gas at high densities. The deficiency in high-density regions results from the lack of the diffuse component feeding giant molecular clouds (Tonnesen & Bryan 2009). The recent work of Ruszkowski et al. (2014) indicates that an accurate description of magnetic fields in models does not significantly change the efficiency of gas stripping, but only explains the formation of the filamentary structures observed in the stripped material.

Smith et al. (2012c) studied the effects induced by ram pressure stripping on the stellar disk and dark matter halo of cluster galaxies. Their simulations indicate that, although the ISM–IGM interaction acts only on the gaseous component, thanks to their mutual gravitational interaction, the gas displacement perturbs the potential well of the galaxy, dragging the stellar disk and the cusp of the dark matter halo off center. The perturbation can also mildly deform and heat the stellar disk. The same team has also simulated the effects of ram pressure stripping on newly formed tidal dwarf galaxies (Smith et al. 2013). Because of their low dark matter content, tidal dwarfs are very fragile systems that can be easily perturbed and even totally destroyed through gas and stellar loss. Consistently with these works, Kronberger et al. (2008a) have shown that a ram pressure stripping event can affect the 2D velocity field of galaxies determined from emission lines. The perturbation is symmetric in a face-on interaction, while can displace the dynamical center of the galaxy in edge-on interactions. The interaction can also increase the activity of star formation in the inner regions where the compressed gas is located (Kronberger et al. 2008b).

Bekki (2009) simulated the effects of halo gas stripping in galaxies of different mass belonging to different environments. This work has shown that halo gas stripping on Milky Way type galaxies is very efficient not only in massive clusters but also in small and compact groups. The removal of gas happens outside-in, producing truncated star forming radial profiles. The stripping process is more rapid in dense environments than in groups, and in low-mass systems with respect to massive galaxies. The same team has also shown that repeated slow encounters within groups are able to transform star forming systems into S0 (Bekki & Couch 2011). These gravitational interactions can trigger the formation of new stars through repetitive starbursts, and at the same time consume the gas reservoir producing gas-poor objects. The resulting systems have lower velocity rotations and higher velocity dispersions than their progenitors. The ram pressure stripping event can either enhance or reduce the activity of star formation depending on the mass of the galaxy, on the inclination of its disk with respect to the orbit and the environment in which the galaxy resides (Bekki 2014). Kawata & Mulchaey (2008) have simulated the effects of gas stripping in groups of virial mass $8 \times 10^{12}\,\mathrm{M}_{\odot}$ and total X-ray luminosity $L_X \simeq 10^{41}\,\mathrm{erg\,s^{-1}}$ on a galaxy of $M_{\mathrm{star}} \simeq 3.4 \times 10^{10}\ \mathrm{M}_{\odot}$. Their N-body/smoothed particle hydrodynamic simulations show that ram pressure stripping is not able to remove the cold gas over the disk of the galaxy, but is sufficient to remove the hot gas located in the halo on time scales of ∼1 Gyr. Because of the lack of new gas feeding star formation, the galaxy quenches its activity in ∼4 Gyr. These conclusions, however, are not confirmed by the simulations of Hester (2006) who identify ram pressure as the most efficient process in stripping the cold gas component even inside groups of galaxies. Stripping of the hot gaseous halos in clusters and groups galaxies have

also been modeled using 3D-hydrodynamical simulations by McCarthy et al. (2008). These simulations indicate that a significant fraction of the hot gas, $\simeq$30 %, can remain in place after a 10 Gyr interaction, thus in contradiction with other works. McCarthy et al. (2008) developed simple analytic models ideally constructed to be included in semi-analytic models of galaxy evolution to reproduce the gas stripping process in high-density environments.

4.3 Formation of dwarf elliptical galaxies via galaxy harassment

Early N-body simulations specially designed to follow the hierarchical growth of clusters and galaxy harassment and to study the possible formation of dwarf elliptical galaxies through the transformation of star forming disks were carried out by Mastropietro et al. (2005). These simulations are designed for a ΛCDM cluster of 10^7 particles with a total mass similar to the Virgo cluster. The simulations indicate that most of the galaxies undergo major structural modifications even at the outskirts of the cluster, with a large fraction of them transforming from late-type rotating systems into dwarf spheroidal hot systems on time scales of a few Gyrs. The effects are, however, most important in the inner 100 kpc of the cluster. The harassed galaxies are more compact and have comparable or higher surface brightness than unperturbed objects, probably because of the formation of bars or grand design spiral arms. The mass loss is important and induces the formation of round galaxies. Harassment also heats the systems, decreasing the rotational velocity-to-velocity dispersion v/σ ratio. Rotation is totally lost only in the most perturbed objects.

More recently, Aguerri & Gonzalez-Garcia (2009) have developed high-resolution N-body simulations to test the tidal stripping scenario for the formation of dE. These simulations studied the perturbation induced to disk galaxies with different bulge-to-disk ratios. They show that, while the bulge is only marginally affected, the disk and the dark matter halo are efficiently perturbed in the outer parts. The scale length of the stellar disk, for instance, can be reduced by 40–50 %. After several fast encounters galaxies can lose up to 50–80 % of their mass and 30–60 % of their luminous matter. Prograde interactions produce stable bars, while retrograde encounters do not. The formation of bars is more important in the absence of bulges. The interaction heats the system decreasing its v/σ ratio. In a recent study, Benson et al. (2014) simulated the effects of different environmental processes (starvation, ram pressure stripping, tidal stirring) on the evolution of dwarf galaxies in Virgo-like clusters. These simulations were principally focused in reproducing the galaxy kinematical properties. Benson et al. (2014) identified tidal stirring induced by the cluster halo on disk galaxies as the most probable process able to reproduce the observed gradient of the angular momentum of dEs with the clustercentric distance to M87 at the center of the Virgo cluster (see Fig. 17).

4.4 Spectro-photometric models of galaxy transformation

Boselli et al. (2006, 2008a,b) have developed 2D chemo-spectrophotometric models of galaxy evolution especially designed to reproduce the perturbations induced by the hostile environment on star forming disks infalling for the first time in rich clusters. These models reproduce two different kinds of perturbations: ram pressure stripping and starvation. The models are based on the chemo-spectrophotometric models of galaxy evolution of Boissier & Prantzos (2000) where disk galaxies are formed in a dark matter halo and form stars following a Schmidt law modulated by the rotation of the galaxy (Boissier et al. 2003).

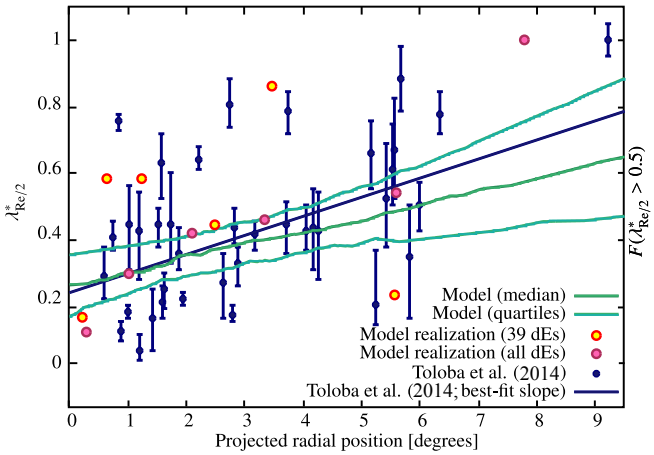

Fig. 17 The distribution of the angular momentum of dEs as a function of the projected distance from M87 (from Benson et al. 2014). © AAS. Reproduced with permission

Calibrated on the Milky Way, the models have two free parameters, the spin parameter λ, which is a dimensionless measurement of the specific angular momentum, and the rotational velocity V_C. Starvation is simulated simply stopping the infall of fresh gas, that the model requires for unperturbed systems to reproduce the observed color and metallicity gradients of nearby galaxies.[18] A stripping event is modeled considering that ram pressure has an intensity varying along the orbit of the galaxy within the cluster, as predicted by the scenario of Vollmer et al. (2001) explicitly designed for Virgo.

These models have been first tuned on a well-known anemic Virgo cluster galaxy undergoing a ram pressure stripping event, NGC 4569 (M90, Boselli et al. 2006), and then extended to dwarf galaxies in the Virgo cluster (Boselli et al. 2008a,b). They show that only ram pressure stripping can reproduce the truncated radial profiles observed in the gaseous component and in the young stellar populations of NGC 4569, ruling out the starvation scenario. They also show that ram pressure stripping can efficiently remove, on very short time scales (≃150 Myr) all the gas in low-mass star forming systems. The lack of gas induces a quenching of the star-formation activity, transforming gas-rich star-forming systems into gas-poor quiescent objects (Fig. 18). This transformation happens on time scales of the order of 0.8–1.7 Gyr. The chemical, structural, spectrophotometric properties of the transformed galaxies are very similar to those of dwarf elliptical galaxies (Boselli et al. 2008a,b). This transformation process would imply that the overall cluster and field luminosity functions are similar, with a mutual inversion of the faint end slope of blue, star forming systems, frequent in low-density regions, and red, quiescent objects, abundant in the core of the cluster, as indeed observed in Virgo and Coma. The models predictions are also consistent with the observed properties of the globular clusters of dwarf ellipticals and their expected progenitors (Boselli et al. 2008a; see however Sanchez-Janssen & Aguerri 2012). These results

[18] We stress that this definition of starvation differs from the one originally proposed by Larson et al. (1980), where the galaxy quenches its activity of star formation once the gas of its halo, generally feeding the disk in unperturbed systems, is removed during the interaction with the hostile environment. In the Boselli et al. models, starvation is a passive process where star formation decreases after gas consumption because of the lack of the infall of pristine gas from the surrounding environment.

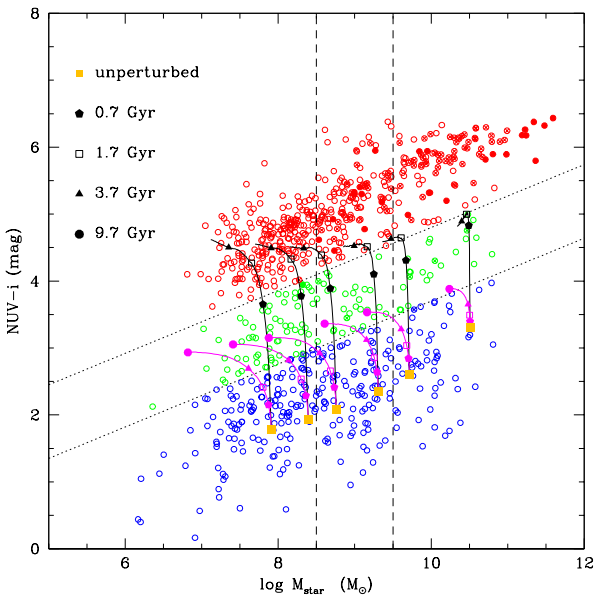

Fig. 18 The extinction corrected $NUV - i$ (AB system) vs. M_{star} relation for all galaxies of the sample, from Boselli et al. (2014a). Filled symbols are for slow rotators, crosses for fast rotators. *Symbols* are color coded for dividing objects in the blue cloud form the green valley and the red sequence. The large *orange filled squares* indicate the models of unperturbed galaxies of spin parameter $\lambda = 0.05$ and rotational velocity 40, 55, 70, 100, 130, 170, and 220 km s^{-1}. The *magenta lines* indicate the starvation models. The *black lines* show the ram pressure stripping models. *Different symbols along the models* indicate the position of the model galaxies at a given look-back time from the beginning of the interaction. Courtesy of ESO

consistently indicate that ram pressure stripping is able to explain the formation of the faint end of the red sequence characterizing rich clusters of galaxies.

4.5 Formation of dwarf galaxies in stripped material

N-body/hydrodynamic simulations of ram pressure stripping events on star forming galaxies in rich clusters show the formation of extended gas tails (350 kpc) in the direction opposite to the motion of the galaxy within the intergalactic medium (Kronberger et al. 2008b; Kapferer et al. 2009). These gas tails are similar to those observed in the periphery of A1367 and Coma by Gavazzi et al. (2001), Yoshida et al. (2008); Yagi et al. (2010), Fossati et al. (2012) in Hα, by Scott et al. (2012) in HI and in X-rays in A3627 (Sun et al. 2010). The same simulations also predict an increase of the total star-formation activity of the galaxy by an order of magnitude, 95 % of which produced in the tail of diffuse gas (Kapferer et al.

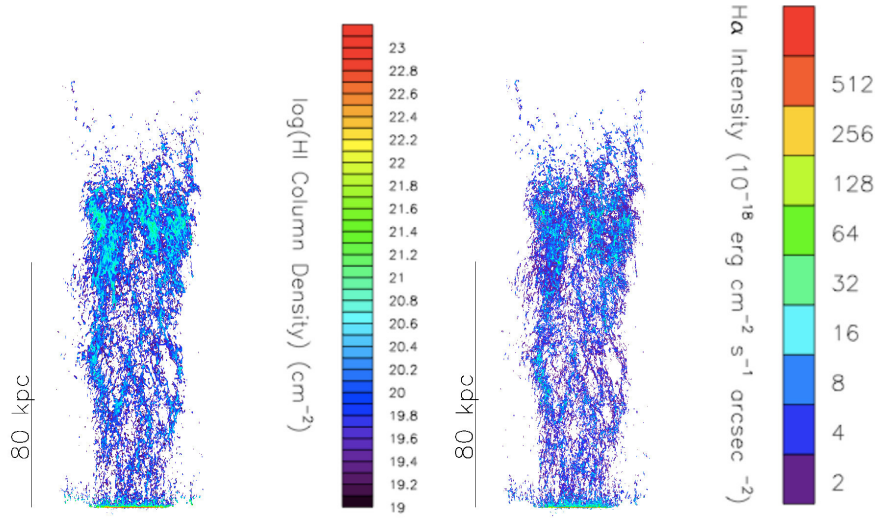

Fig. 19 Projections of the HI column density (left) and of the Hα surface density (right) in the ram pressure stripped gas for a model galaxy with star formation and feedback, adapted from Tonnesen & Bryan (2012). A small amount of star formation can take place in the highest column density regions of the HI gas stripped during the interaction out to 80 kpc from the disk of the galaxy. Reproduced with permission of Oxford University Press

2009). These results were later questioned by Tonnesen & Bryan (2012) who showed, using high-resolution adaptive mesh simulations, that gas stripping produces a truncation of the star forming disk on time scales of a few hundreds million years. They show that there is a moderate increase of the star formation in the bulge but without a starburst phase. They also show that the star formation in the tail is low, and any contribution to the intercluster light, if present, is likely to be very small (see Fig. 19). The difference in the results between Tonnesen & Bryan (2012) and Kapferer et al. (2009) comes mainly from the nature of the two different codes and only marginally on the adopted conditions (Tonnesen & Bryan 2012). Consistently with Tonnesen & Bryan (2012), Yamagami & Fujita (2011) predict that in the absence of magnetic field, Kelvin–Helmholtz instabilities destroy molecular clouds, preventing the formation of new stars in the tails of stripped gas.

Observations seem more consistent with the prediction of Tonnesen & Bryan (2012) and Yamagami & Fujita (2011). Indeed, there are only a few examples of cluster galaxies with major ongoing star-formation events in the stripped material far from the galaxy disk. Typical examples are IC 3418 in Virgo (Hester et al. 2010; Fumagalli et al. 2011; Kenney et al. 2014), ESO137-001 in A3627 (Sun et al. 2007; Jachym et al. 2014; Fumagalli et al. 2014), and two massive objects in two clusters at $z \simeq 0.2$ (Cortese et al. 2007). The extended tails of ionized gas observed in the Hα images of galaxies in nearby clusters (Gavazzi et al. 2001; Kenney et al. 2008; Yoshida et al. 2008; Yagi et al. 2010; Fossati et al. 2012; Jachym et al. 2014) are only marginally associated with major star-formation events in the tails. In the Virgo cluster there are also evident cases of galaxies with extended HI tails but without any associated star-formation event (Boissier et al. 2012), or objects where the outplanar star-formation process is happening only very close to the galaxy disk (Abramson et al. 2011).

5 Observations vs. models: a new evolutionary picture

5.1 The Virgo cluster

The comparison of the observational results obtained so far with model predictions can be used to reconstruct the evolutionary picture that gave birth to the dwarf quiescent galaxies inhabiting nearby clusters that form the faint end of the red sequence. Multifrequency data are critical for this purpose since they provide us with a complete and coherent view of the undergoing process and of its effect on galaxy evolution (e.g. Boselli 2011). We can first apply the exercise to the Virgo cluster. Here, indeed, multifrequency data spanning the whole range of frequencies are available for galaxies down to stellar masses of $\sim 10^7$ M$_\odot$. At the same time, most of the available models and simulations have been carried out with the aim of reproducing the physical conditions undergone by galaxies located in clusters with characteristics similar to those of Virgo.

Observations and models consistently indicate that dwarf elliptical galaxies might have been formed by the transformation of low-luminosity late-type systems recently entered the Virgo cluster once they have lost their gaseous content during the interaction with the hostile cluster environment, as first proposed by Boselli et al. (2008a,b). The most plausible physical process responsible for this transformation is the ram pressure $\rho_{\rm ICM} V^2$ exerted by the hot and dense intracluster medium (where $\rho_{\rm ICM}$ is its density) on galaxies moving at high velocity (V) within the cluster. Both models and observations indicate that this ram pressure is able to overcome the gravitational forces keeping the gas anchored to the potential well of the galaxy, $G\Sigma_{\rm gas}\Sigma_{\rm star}$, where G is the gravitational constant and $\Sigma_{\rm gas}$ and $\Sigma_{\rm star}$ are the gaseous and stellar surface density, respectively (Gunn & Gott 1972). This is particularly true in dwarf systems, where the gravitational potential well is shallower than in massive galaxies. Ram pressure stripping easily removes both the atomic (e.g. Cayatte et al. 1990; Solanes et al. 2001; Gavazzi et al. 2005, 2013a) and in the strongest cases the molecular gas phases (Fumagalli et al. 2009; Boselli et al. 2014b), as well as the associated dust (Cortese et al. 2010, 2012a,b). Models and observations consistently indicate that ram pressure stripping is efficient even outside the virial radius of the cluster (Roediger & Hensler 2005; Roediger & Bruggen 2006, 2007; Boselli & Gavazzi 2006; Tonnesen & Bryan 2009; Cen et al. 2014). The higher dispersion in the velocity distribution of star-forming systems with respect to that of massive ellipticals definitely shows the presence of gas rich systems infalling in the Virgo cluster (Boselli et al. 2008a, 2014a).

The stripping process is quite rapid since it is able to remove most of the gas content on time scales of ~1.5 Gyr (Roediger & Bruggen 2007; Tonnesen & Bryan 2009). This time scale even reduces to 100–200 Myr in dwarf systems because of their weak restoring forces (Boselli et al. 2008a). Some gas retention, with the associated dust (de Looze et al. 2010, 2013), might be present in the core of the stripped galaxies where the gravitational potential well is at its maximum. This gas might feed star formation up to more recent epochs, and thus be at the origin of the blue centers observed in the most massive dwarf ellipticals ($\sim 10^{9.5-10} M_\odot$) (Lisker et al. 2006b; Boselli et al. 2008a; Michielsen et al. 2008; Paudel et al. 2011). Indeed, gas removal is an outside-in process able to perturb only the gaseous component not affecting the stellar component, if not indirectly via the star-formation process (Boselli et al. 2006). The stripped galaxies often show in their morphology several remnants of their past spiral origin, such as grand design spiral arms, disks, and bars (Jerjen et al. 2000; Geha et al. 2003; Lisker et al 2006a,b; Lisker & Fuchs 2009). They also conserve their angular momentum, showing rotation curves similar to those observed in spiral galaxies of similar luminosity (Toloba et al. 2009, 2011, 2014b). Because of the lack of gas,

the star formation stops, making galaxies redder and redder (Boselli et al. 2008a, 2014a; Cortese & Hughes 2009; Hughes & Cortese 2009; Gavazzi et al. 2013a). When plotted in a color magnitude diagram, they leave the blue sequence, cross the green valley and become red, quiescent systems. The time scale for this transformation is only slightly longer than the time scale for the gas stripping (Boselli et al. 2008a, 2014a). A rapid quenching of the star-formation activity is also indicated by the presence of several dwarf ellipticals such as VCC 1499 (see Sect. 1) in a post-starburst phase.[19] The structural properties of the newly formed dwarf elliptical galaxies, as well as those of their relative globular cluster content, are fully consistent with those of their star forming progeny (Boselli et al. 2008a,b; see, however, Sanchez-Janssen & Aguerri 2012). There is strong and consistent evidence that the kinematical, structural, and spectrophotometric properties of dwarf ellipticals within Virgo tightly depend on their position within the cluster. Indeed, the most roundish (Lisker et al. 2009), pressure-supported systems (Toloba et al. 2009, 2011) dominated by old stellar populations in their center (Michielsen et al. 2008; Paudel et al. 2010a, 2011) are located close to the cluster core, while the disky, rotationally supported systems, dominated by younger stellar populations in their center, are predominantly situated in the outskirts of the Virgo cluster.

The statistical properties of the Virgo cluster galaxies are also consistent with this picture. The shape of the optical and UV luminosity functions, and in particular their faint end slope, are very similar to those observed in the field once low surface brightness galaxies are considered (Rines & Geller 2008; Boselli et al. 2011; Ferrarese et al., in prep.). There is just an inversion of the relative contribution of star forming and quiescent galaxies, the former dominating in low-density regions, the latter typical of rich environments, as indeed expected in such a scenario. We recall, however, that both the GUViCS UV (Boselli et al. 2011) and the NGVS optical (Ferrarese et al., in prep.) luminosity functions have been determined for the central regions of the cluster and thus do not sample any possible radial variation (steepening of the faint end in the cluster periphery) already observed in other nearby clusters (Popesso et al. 2006; Barkhouse et al. 2007, 2009).

The comparison of models with observations strongly favors a soft interaction of galaxies with the hot intergalactic medium (ram pressure) rather than more violent phenomena such as tidal interactions or galaxy harassment for several reasons. The most important one is that gravitational interactions remove a significant fraction of the stellar component, producing lower luminosity objects with systematically truncated stellar disks (Mastropietro et al. 2005; Aguerri & Gonzalez-Garcia 2009). The interaction would also significantly increase stochastic motions and reduce ordered motions, thus finally decreasing v/σ (Mastropietro et al. 2005; Aguerri & Gonzalez-Garcia 2009). The observed structural properties of dwarf galaxies are more consistent with those of star-forming systems stripped of their gas by ram pressure stripping rather than those of harassed galaxies (Boselli et al. 2008b). Furthermore, efficient gravitational perturbations are quite rare given the high-velocity dispersion of the cluster. We thus expect that harassment requires long time scales for galaxy transformation, longer than the observed evolution with redshift of the faint end of the CMR (see Sect. 5.4). We can also expect that strong gravitational interactions, through tidal disruption and tidal galaxy formation, should significantly modify the shape of the luminosity function (Popesso et al. 2006; Barkhouse et al. 2007; de Filippis et al. 2011). As previously mentioned, the observations do not show any systematic difference in the luminosity function of Virgo and the field. At the same time, the detailed observations of the few cluster galaxies with clear signs

[19] The definition of post-starburst does not necessarily imply there was a particularly acute starburst phase, but that a normal star-formation phase was abruptly interrupted.

of an undergoing perturbation do not show the formation of intermediate mass objects, but rather the formation in the stripped material of very small, compact blobs of stellar mass $\sim 10^3 - 10^6$ $M_\odot$ (Yoshida et al. 2008; Fumagalli et al. 2011; Arrigoni Battaia et al. 2012; Yagi et al. 2013). This phenomenon of galaxy disruption/formation does not seem to be very frequent and is thus quite unlikely that it is able to modify the shape of the luminosity function in the observed stellar mass range. Furthermore, the output of this process are not low surface brightness, extended systems as those dominating the faint end of the luminosity function and of the CMR, but rather compact sources much more similar to UCD galaxies (yet of lower mass; Arrigoni Battaia et al. 2012).

All the evidence described above, however, does not necessarily rule out the hypothesis that gravitational perturbations might play an important role on those galaxies that entered the cluster long time ago or have been even formed within it. On long time scales, galaxy harassment can heat the perturbed systems, producing roundish, pressure-supported objects such as those observed in the core of the cluster by Lisker et al. (2007, 2009). These galaxies, that have on average a velocity distribution similar to the Gaussian distribution drawn by the massive virialized ellipticals, are indeed characterized by older stellar populations (Michielsen et al. 2008; Paudel et al. 2010a, 2011) and lower v/σ (Toloba et al. 2009, 2011; Boselli et al. 2014a) than their disky dominated counterparts at the periphery of the cluster. Furthermore, the beautiful systematic work of Lisker, Janz and collaborators, have undoubtedly shown that dwarf elliptical galaxies are not an homogeneous class of objects, but rather present different structures remnants of different possible origins (Lisker 2009; Janz et al. 2012, 2014). We can also add that chemo-spectrophotometric models of galaxy evolution expressly conceived to take into account the perturbations induced by the cluster environment ruled out the hypothesis that starvation, or strangulation, is at the origin of the observed properties of dwarf (and giant) gas-poor galaxies in clusters (Boselli et al. 2006, 2008a). We recall, however, that these models simulate starvation by stopping the infall of pristine gas, as already noted in Sect. 4.4. In the original definition of Larson et al. (1980) starvation is a more aggressive process, where the interaction of galaxies with the hot and dense intracluster medium removes the hot gaseous halos of galaxies, a process that is much more similar to the ram pressure stripping considered here.

A still open question is the range of stellar mass where this transformation process is efficient. Given the tight relation between stellar mass and restoring forces on galaxy disks, we expect the gas stripping process to be less efficient in massive objects (Boselli et al. 2008a). Here an important fraction of the atomic and molecular gas can still be retained on the inner disk, feeding star formation. Total gas stripping might occur only after several crossings of the cluster (Boselli et al. 2014b). It is thus possible in this scenario that the most massive ETGs inhabiting the cluster have been formed through major merging events, as indeed suggested by kinematical arguments (Cappellari et al. 2011a,b; Boselli et al. 2014a). It would be interesting to extend the studies of the main scaling relations and see whether the possible presence of strong discontinuities, as claimed by Kormendy et al. (2009) and Kormendy & Bender (2012), or continuity (Graham & Guzman 2003; Gavazzi et al. 2005; Ferrarese et al. 2006; Misgeld et al. 2008, 2009; Misgeld & Hilker 20011; Smith Castelli et al. 2013) can shade light on this specific point.

Within this evolutionary picture we see only one apparent inconsistency. The cosmological simulations by Weinmann et al. (2011) and Lisker et al. (2013) especially tuned to reproduce the properties of the Virgo cluster seem to indicate that dwarf elliptical galaxies in local clusters such as Virgo might have been processed early and continuously in groups and in the cluster halo and are thus not LTGs recently transformed in quiescent systems. There are, however, a few indications that these semi-analytic models fails to reproduce several

statistical properties of local clusters. Among these, the most evident is that they overestimate the color and the number of red objects, suggesting that in semi-analytic models the effects of the environment are still not optimized (Weinmann et al. 2011).

5.2 Other clusters

Are these results consistent with what observed in other nearby clusters? The multifrequency observations of Coma, A1367, and the Shapley supercluster confirm this scenario. All observations indicate that the fraction of gas-rich star-forming galaxies continuously increases with clustercentric distance up to a few virial radii (Rines et al. 2005; Gavazzi et al. 2013b), and that, on average, gas-poor late-type systems typical of high-density environments populate the green valley in between the blue cloud and the red sequence. The observations also indicate that dwarf elliptical galaxies in the infalling regions at the periphery of these rich clusters have, on average, younger stellar populations than those located close to the cluster core (Smith et al. 2006, 2008, 2009, 2012a), often with characteristic spectra indicating a recent abrupt truncation of their star-formation activity (Poggianti et al. 2004; Gavazzi et al. 2010). There is also evidence that some of these low-mass quiescent systems have spiral arms (Graham et al. 2003) and residual star formation in their center (Haines et al. 2008). The physical properties of star-forming and quiescent dwarf galaxies in other nearby clusters are thus similar to those observed in Virgo.

As for Virgo, we expect that ram pressure stripping is the most probable process responsible for the observed trends. In rich clusters such as Coma the density of the intracluster medium is, on average, a factor of ten higher than in less relaxed clusters such as Virgo. The velocity dispersion of galaxies also increases with the mass of the cluster; it is thus natural that the efficiency of ram pressure stripping, which varies as $\rho_{\rm ICM}V^2$, is higher in these environments than in Virgo. On the contrary, the increase of the velocity dispersion of the cluster makes gravitational perturbations less efficient just because the time during which two galaxies can interact becomes shorter (Boselli & Gavazzi 2006). There are also a few spectacular observations that confirm this result. Besides the aforementioned FGC1287 in the outskirts of A1367 (Scott et al. 2012), the detection of several gas-rich galaxies at $\sim$ 1 virial radius with extended Hα tails in Coma and A1367 (Gavazzi et al. 2001; Yagi et al. 2007, 2010; Yoshida et al. 2008, 2012; Fossati et al. 2012) has indeed shown that gas stripping via ram pressure can also remove the ionized gas component. At the same time, the X-ray and CO observations of ESO 137-001 in A3627 have indicated that the hot and the molecular gas components can also be removed (Sun et al. 2007; Jachym et al. 2014). Ram pressure stripping seems thus more important than previously thought. This statement is consistent with the most recent hydrodynamical simulations indicating that the ram pressure stripping process is more efficient whenever a multiphase ISM medium (atomic plus molecular gas) is considered (Tonnesen & Bryan 2009). Other simulations also indicate that ram pressure stripping is efficient to remove gas in galaxies up to $\sim$3 virial radii. Altogether these results have proven that ram pressure stripping is still active well outside the virial radius, making it the most plausible process responsible for the radial variation of the gas stripping and following quenching of the star-formation activity observed in nearby clusters.

Not all pieces of evidence, however, rule out gravitational interactions as a possible process able to modify the evolution of cluster galaxies. In a recent work, for instance, Poggianti et al. (2013) discovered a population of compact objects analogue to those found at high redshift, three times more frequent in clusters than in the field, accounting for $\sim$12 % of the massive ($M_{\rm star} > 10^{10}$ M$_\odot$) galaxy population in nearby clusters. These objects, mainly

lenticulars or ellipticals, have been probably shaped by gravitational interactions able to truncate stellar disks. There are also some inconsistencies with the observation of the optical luminosity function of nearby clusters. If the results of Popesso et al. (2005) and Cortese et al. (2008b), indicating that the cluster luminosity function is significantly steeper than in the field, (with a faint end slope in the fitted Schechter function of $-2.1 \leq \alpha \leq -1.6$) are confirmed, other gravitational processes such as harassment and tidal disruption should be invoked. We recall, however, that these results should still be confirmed observationally, in particular because they might suffer from the quite uncertain background subtraction technique (Rines & Geller 2008). In any case, it is also conceivable that, given the very different nature of Virgo and Coma or other massive clusters, the former being spiral rich and still under formation, the latter quite relaxed and spiral poor, the relative weight of the different physical process acting on galaxies might significantly change. If observations and simulations mainly suggest that the dynamical interactions between galaxies and the hot intracluster medium are probably modulating the evolution of galaxies in the present epoch, this might not have been the case in the past, when pre-processing was probably more important (e.g. Dressler 2004; Boselli & Gavazzi 2006). Gravitational perturbations in infalling groups are rare in the present epoch: the blue infalling group in A1367 is indeed the only known case in the local universe (Sakai et al. 2002; Gavazzi et al. 2003b; Cortese et al. 2006b). Furthermore, the luminosity function, in particular in the optical bands, gives a view of the cumulative evolution of galaxies and thus might be not representative of a recent evolution.

5.3 Lower density environments

It is now interesting to determine the range of galaxy density within which this evolutionary process holds. The works of Haines et al. (2008), Gavazzi et al. (2010, 2013b), and Rasmussen et al. (2012a) are crucial for this purpose. In particular, Gavazzi et al. (2010) have shown (see Fig. 13) that while the bright end of the red sequence is already fully defined in all kinds of environments, the faint end is present only for densities $\delta_{1,1,000} > 4$, where $\delta_{1,1,000}$ is the 3D density contrast defined as

$$\delta_{1,1,000} = \frac{\rho - \langle\rho\rangle}{\langle\rho\rangle} \tag{1}$$

ρ is the local number density and $\langle\rho\rangle = 0.05$ gal h^{-1} Mpc^{-3} is the mean number density measured in the Coma/A1367 supercluster region.[20] This threshold in local number density of $\delta_{1,1,000} > 4$ roughly corresponds to the density observed in groups with more than 20 objects and velocity dispersion of $\sim$200 km s^{-1}. The lack of red sequence faint quiescent galaxies in the field has been later confirmed on strong statistical basis by Wilman et al. (2010) and Geha et al. 2012. Kilborn et al. (2009), Fabello et al. (2012), Gavazzi et al. (2013b), and Catinella et al. (2013) have shown that LTGs in medium-density environments such as groups also suffer from gas deficiency. The lack of gas quenches the activity of star formation, making, on average, redder galaxies (Gavazzi et al. 2013b). Wilman et al. (2010), using a large sample of SDSS galaxies in different density environments, have shown that galaxies become red only once they have been accreted into halos of a certain mass.

[20] The local number density ρ around each galaxy is measured within a cylinder of radius 1 h^{-1} Mpc and half-length 1,000 km s^{-1}.

Rasmussen et al. (2012a), on the other hand, have clearly shown that the quenching of the star-formation activity is stronger in galaxies with stellar mass $M_{\rm star} < 10^{9.2}\,{\rm M}_{\odot}$.

ROSAT and *Chandra* observations have shown that about half of the optically selected nearby groups are characterized by a diffuse X-ray emission, similar to clusters of galaxies (Mulchaey & Zabuldoff 1988; Mulchaey 2000; Mulchaey et al. 2003; Osmond & Ponman 2004; Rasmussen et al. 2008; Sun et al. 2009). The X-ray emission, which is typical of those groups dominated by an ETG, generally extends out to less than half of the virial radius. They are characterized by gas densities of $n_0 \sim 10^{-2}-10^{-3}\,{\rm cm}^{-3}$ and velocity dispersions of $\sigma \sim 150-400\,{\rm km\,s}^{-1}$ (Rasmussen et al. 2008). It is thus conceivable that ram pressure stripping is also acting on galaxies in these medium density systems (Kantharia et al. 2005; Verdes-Montenegro et al. 2007; Sengupta et al. 2007; McConnachie et al. 2007; Jeltema et al. 2008). Its efficiency, however, significantly drops since both the mean density of the intergalactic medium and the velocity dispersion are significantly smaller than in cluster galaxies (Kawata & Mulchaey 2008). In dwarf systems, however, the ram pressure stripping process can still be active given their shallow gravitational potential well, as suggested by the results of Rasmussen et al. (2012a). Indeed, through a statistical study of the spectroscopic properties of a large sample of nearby, ETGs, Thomas et al. (2010) have shown that the impact of the environment on the star-formation history of galaxies increases with decreasing galaxy mass. At the same time, in groups the role of gravitational perturbations can be more important than in rich systems just because the duration of the interactions is longer (Kilborn et al. 2009). The hydrodynamical simulations of Bekki & Couch (2011), indeed, have shown that repeated slow encounters within groups are able to transform star forming systems into lenticular galaxies. It is thus possible that the same process modulates the evolution of lower mass systems. On the other hand, the analysis of a large sample of galaxies in groups using SDSS data done by van den van den Bosch et al. (2008) seems to indicate starvation or strangulation as the most probable process quenching the activity of star formation of late-type systems and thus forming the red sequence. This last conclusion, however, is under debate since it is based on the assumption that harassment and ram pressure stripping are efficient only in massive systems, an assumption not fully supported by the results presented in this review. We recall, however, that the simulations of Kawata & Mulchaey (2008) indicate that the total hot halo gas of galaxies of intermediate mass can be removed on time scales of ∼1 Gyr. The lack of new gas feeding the star-formation process quenches the activity of these objects. We also remind that other processes have been proposed in the literature to remove the gas and quench the activity of star formation of dwarf systems in small groups of galaxies similar to the Local group. Among these, we can mention tidal stirring (Mayer et al. 2001a,b), or the combination of tidal interactions and ram pressure stripping exerted on dwarf satellites during their crossing of the halo of massive galaxies (Mayer et al. 2006). Regardless of the very nature of the gas stripping process, we expect that the lack of gas feeding star formation quenches the activity and makes galaxies in groups redder, thus populating the faint end of the red sequence.

5.4 Dependence on redshift

The identification of the process at the origin of the faint end of the red sequence can be further constrained by comparing the time scale for quenching the activity of star formation, transforming blue galaxies into red systems, and the infall rate in nearby clusters, with the evolution of the red sequence as a function of redshift. This exercise has been done for the first time by Boselli et al. (2008a) and later revisited by Gavazzi et al. (2013a,b). Boselli et

al. (2008a) used their own chemo-spectrophotometric models of galaxy evolution to calibrate different indicators necessary to quantify the lookback time since the beginning of the interaction. In this way they identified four different indices: the Hα emission line equivalent width and the HI-deficiency parameter are sensitive to short time scales (∼200 Myr), while the equivalent width of the Hβ absorption line and the FUV-H colour index are sensitive to significantly longer lookback times (∼1 Gyr). By determining the fraction of dwarf elliptical galaxies still undergoing the transformation process as indicated by these four indices in the whole dE Virgo population, Boselli et al. (2008a) deduced that the infall rate of dwarf galaxies in Virgo is of the order of 300 objects Gyr^{-1}. Following similar arguments, Gavazzi et al. (2013a) determined infall rates of ∼300 to 400 Gyr^{-1} galaxies in Virgo and of 100 galaxies Gyr^{-1} of mass $M_{\rm star} > 10^9$ M$_\odot$ in Coma. These are important rates considering that the total number of dwarf Virgo members in the same luminosity range is ∼650 and implies that the faint end of the red sequence has been formed in the last ∼2 Gyr (corresponding to $z = 0.16$ in a $H_0 = 70\,{\rm km\,s^{-1}\,Mpc^{-1}}$, $\Omega_m = 0.3$, and $\Omega_\lambda = 0.7$ cosmology) if we assume that this rate did not change significantly with time (Boselli et al. 2008a).

The most recent studies of the CMR and of the luminosity function in clusters at different redshifts can be used for a direct comparison with this result. Since the work of Kodama et al. (2004) and De Lucia et al. (2004) there is a growing evidence that the fraction of luminous-to-faint galaxies on the red sequence significantly decreased since $z = 0.8$ (Fig. 20; De Lucia et al. 2007, 2009; Stott et al. 2007, 2009; Gilbank & Balogh 2008; see however Andreon 2008). Stott et al. (2007) determined that the number of dwarf galaxies on the red sequence increased by a factor of 2.2 since $z = 0.5$ (4 Gyr), a number roughly consistent with that determined from the infall rate of galaxies in Virgo (Boselli et al. 2008a; Gavazzi et al. 2013a). Jaffe et al. (2011), by analyzing the shape of the CMR traced by galaxies selected according to morphological criteria, have shown that the CMR was already formed in clusters at redshift $0.4 < z < 0.8$. They noticed, however, the presence of several low luminosity objects with bluer colors than those of the mean CMR, indicating that these galaxies have reached the red sequence later in time than more massive galaxies. By comparing the fraction of red dwarf galaxies with clear signs of a post-starburst activity ('$k+a$') with the infalling rate, De Lucia et al. (2009) have shown that not all dwarf galaxies have moved from the blue cloud to the red sequence after having passed a post-starburst phase. They have thus concluded that the transformation process that gave birth to the faint end of the red sequence is not always rapid, but can mildly and continuously change the galaxies properties with time. Using a different set of data of high redshift galaxies, Bolzanella et al. (2010) suggested that the environmental mechanisms of galaxy transformation start to be effective only below $z = 1$. Furthermore, they indicated that the migration from the blue cloud to the red sequence occurs on a shorter timescale than the transformation from disk-like morphologies to ellipticals, consistently with that observed in the local universe (presence of spiral arms in Virgo and Coma dE, see Sect. 3.6) (Giodini et al. 2012; Mok et al. 2013; Vulcani et al. 2013). It has been shown that the fraction of galaxies in dense environments at $z = 0.7$ located in between the red and the blue sequence of the color–magnitude relation, thus of objects probably undergoing the transformation process, increases with decreasing luminosity (Cassata et al. 2007), as expected in the proposed scenario. There are also several indications that the faint end of the luminosity function of red cluster galaxies has been formed only after $z = 0.6$ (Harsono & de Propris 2007; Gilbank et al. 2008; Rudnick et al. 2009, 2012; Lemaux et al. 2012; see, however Crawford et al. 2009; de Propris et al. 2013). More locally, the work of Hansen et al. (2009) based on the photometric properties of galaxies in group and clusters at redshift $0.1 < z < 0.3$ has shown that, while the lumi-

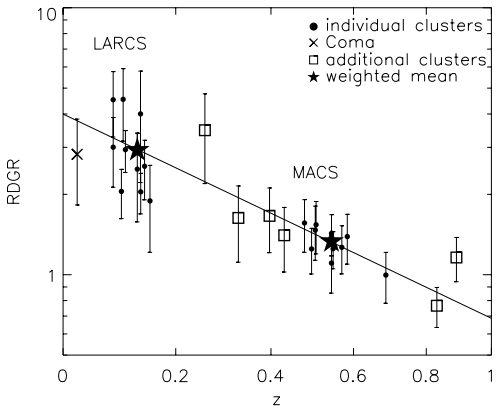

Fig. 20 The variation in the red sequence of the dwarf to giant number ratio as a function of the redshift, from Stott et al. (2007). Dwarf elliptical galaxies have been formed mainly at recent epochs. © AAS. Reproduced with permission

nosity function of blue and red satellites is only weakly dependent on the cluster richness for masses above 3×10^{13} $M_{\odot}$, the mix of faint red and blue galaxies changes dramatically.

Overall, although controversial results have been reported, most of the observational evidence suggests that the faint end of the red sequence has been formed only at relatively recent epochs. It might be more challenging to see whether the physical process at the origin of this transformation in the past was the same as the one identified in the local universe (ram pressure stripping). Simulations indicate that the present day rich clusters have been formed by the aggregation of smaller structures and that ∼40 % of the galaxies in local clusters have been accreted through groups (Gnedin 2003; McGee et al. 2009; De Lucia et al. 2012). It is thus conceivable that galaxies have been processed during their membership to these systems before entering in the cluster (pre-processing, Dressler 2004; Vijayaraghavan & Ricker 2013; Dressler et al. 2013). There is also some evidence that clusters were denser at high z than in the local universe (Poggianti et al. 2010). It is thus possible that gravitational

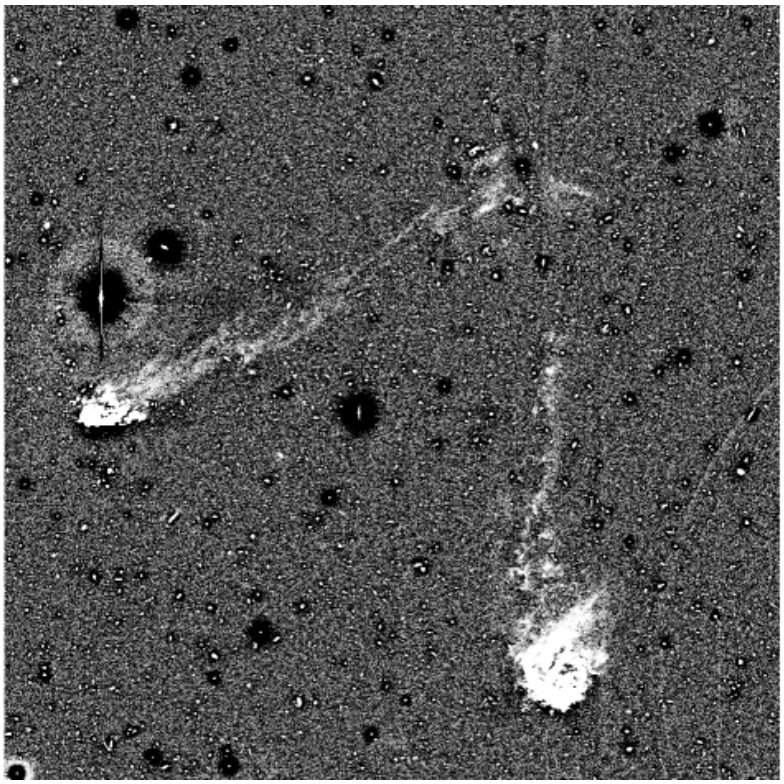

Fig. 21 High contrast representation of the Hα NET frame obtained with the Suprime-Cam at the Subaru telescope (4 hours exposure) zoomed on a 10x10 arcmin^2 region containing galaxies 97073 and 97079 (compare with Figure 1), showing tails of ionized gas exceeding 100 kpc in length

interactions played a more important role in shaping dwarf galaxy evolution in the past than in the local universe. The short time scale for the assembly of the faint end of the red sequence (~4 Gyr), however, favors rapid processes such as ram pressure stripping rather than harassment, whose time scale is longer given that multiple encounters are required. The interesting works of Poggianti and collaborators also favor this scenario. By studying the spectral properties of cluster galaxies at redshift $0.4 < z < 0.8$, Poggianti et al. (2009) have shown that the fraction of post-starburst galaxies increases with the velocity dispersion of the cluster, suggesting that the process at the origin of their transformation is related to the intracluster medium. Consistently with this scenario, Dressler and collaborators concluded that massive ellipticals have been formed by early major merging events within the groups accreting the cluster, while lenticulars more recently by less violent processes. This view is also consistent with the most recent multifrequency observations of the Virgo cluster (Boselli et al. 2014a).

6 Concluding remark

In spring 2014 we took a 1 deg^2 deep (4 h exposure) Hα image of A1367 using Suprime-Cam at the Subaru telescope, in collaboration with Michintoshi Yosida and Masafumi Yagi.

Moreover, we obtained one field at the NW periphery of the Coma cluster which, added to the two fields previously obtained by Yagi et al. (2010) with the same instrument, brings to 1.5 sq. deg. the area surveyed in this cluster at similar depth. Figure 21 speaks for itself. It contains a detail of the A1367 field, zoomed on two of the galaxies highlighted in Fig. 1. The gray scale represents the intensity of the Hα + N[II] lines after a preliminary subtraction of the stellar continuum. The figure shows ionized gas (no stars) trailing behind the two low-mass galaxies ($M_{\rm star}$ $10^{9.3,9.5}$ $M_\odot$) with approximately 75 (97073) and 100 kpc (97079) projected length. It cannot be excluded that the two galaxies suffered from a close encounter at the location where the two tails seem to cross each other. Nevertheless they dramatically witness gas loss due to ram-pressure.

In total we covered 36 LTGs in A1367 and 28 in the Coma cluster. The preliminary result of the survey is that at least 24 (perhaps 27) of them, i.e. 40 %, present a cometary Hα tail. In other words, roughly one out of two of the star forming galaxies in the two clusters shows signs of an ongoing ram pressure interaction. This confirms that ram pressure is a quick phenomenon, that replenishment of fresh gas-rich galaxies is currently taking place in the clusters belonging to the Great Wall and that environmental transformations are indeed ubiquitous. If this rate is representative of other clusters, we predict that future Hα surveys of similar depths (few 10^{-18} erg cm^{-2} s^{-1} arcsec^{-2}) of the Virgo cluster would lead to the detection of several hundred LTGs showing cometary structures, especially in dwarf systems. The recent availability of Hα filters matching the field of view of MegaCam at the CFHT will make such survey feasible in the near future. Another major breakthrough for unveiling at the same time the kinematics and the chemistry of these systems will certainly be provided by the wide-field integral-field units that are becoming available at 10 m class telescopes (e.g. MUSE at VLT: Fumagalli et al. 2014 and KCWI at Keck) and by ALMA for disclosing the study of the gas in the molecular phase.

Acknowledgements We wish to thank Massimo Dotti, Matteo Fossati, Michele Fumagalli, and Elisa Toloba for their comments on the manuscript and Yannick Roehlly for his help in the preparation of the illustrations. G.G wishes to thank Michitoshi Yoshida and Masafumi Yagi for their permission to use the Halpha map in Fig. 21 prior to publication. The authors would like to thank L. Cortese, K. Rines, R. Smith, T. Lisker, E. Toloba, S. Tonnesen, and J. Stott for allowing reproducing their published figures. During the writing of this review we made extensive use of the GOLDMine database (Gavazzi et al. 2003a) and of the NASA/IPAC Extragalactic Database (NED) which is operated by the Jet Propulsion Laboratory, California Institute of Technology, under contract with the National Aeronautics and Space Administration. Funding for the SDSS and SDSS-II has been provided by the Alfred P. Sloan Foundation, the Participating Institutions, the National Science Foundation, the U.S. Department of Energy, the National Aeronautics and Space Administration, the Japanese Monbukagakusho, and the Max Planck Society, and the Higher Education Funding Council for England. The SDSS Web site is *http://www.sdss.org/*. The SDSS is managed by the Astrophysical Research Consortium (ARC) for the Participating Institutions. The Participating Institutions are the American Museum of Natural History, Astrophysical Institute Potsdam, University of Basel, University of Cambridge, Case Western Reserve University, The University of Chicago, Drexel University, Fermilab, the Institute for Advanced Study, the Japan Participation Group, The Johns Hopkins University, the Joint Institute for Nuclear Astrophysics, the Kavli Institute for Particle Astrophysics and Cosmology, the Korean Scientist Group, the Chinese Academy of Sciences (LAMOST), Los Alamos National Laboratory, the Max-Planck-Institute for Astronomy (MPIA), the Max-Planck-Institute for Astrophysics (MPA), New Mexico State University, Ohio State University, University of Pittsburgh, University of Portsmouth, Princeton University, the United States Naval Observatory, and the University of Washington.

References

1. Abazajian KN et al (2009) ApJS 182:543
2. Abramson A, Kenney JDP, Crowl HH et al (2011) AJ 141:164

3. Aguerri J-A-L, González-García A-C (2009) A&A 494:891
4. Ahn CP, Alexandroff R, Allende Prieto C et al (2012) ApJS 203:21
5. Ahn CP, Alexandroff R, Allende Prieto C et al (2014) ApJS 211:17
6. Akimoto F, Kondou K, Furuzawa A, Tawara Y, Yamashita K (2003) ApJ 596:170
7. Andrade-Santos F, Nulsen PEJ, Kraft RP et al (2013) ApJ 766:107
8. Andreon S (2008) MNRAS 386:1045
9. Arnaud M, Aghanim N, Gastaud R et al (2001) A&A 365:L67
10. Arrigoni Battaia F, Gavazzi G, Fumagalli M et al (2012) A&A 543:A112
11. Bacon R, Copin Y, Monnet G et al (2001) MNRAS 326:23
12. Bahé Y-M, McCarthy I-G, Crain R-A, Theuns T (2012) MNRAS 424:1179
13. Bahé YM, McCarthy IG, Balogh ML, Font AS (2013) MNRAS 430:3017
14. Bai L, Rieke GH, Rieke MJ et al (2006) ApJ 639:827
15. Bai L, Rieke GH, Rieke MJ, Christlein D, Zabludoff AI (2009) ApJ 693:1840
16. Balogh ML, Navarro JF, Morris SL (2000) ApJ 540:113
17. Balogh ML, Baldry IK, Nichol R et al (2004) ApJl 615:L101
18. Barkhouse WA, Yee HKC, López-Cruz O (2007) ApJ 671:1471
19. Barkhouse WA, Yee HKC, López-Cruz O (2009) ApJ 703:2024
20. Bekki K (2009) MNRAS 399:2221
21. Bekki K (2014) MNRAS 438:444
22. Bekki K, Couch WJ (2011) MNRAS 415:1783
23. Benson A, Toloba E, Mayer L, Simon J, Guhathakurta P (2014) ApJ. (in press)
24. Berlind AA, Blanton MR, Hogg DW et al (2005) ApJ 629:625
25. Binggeli B, Cameron LM (1991) A&A 252:27
26. Binggeli B, Sandage A, Tammann GA (1985) AJ 90:1681
27. Blanton MR, Moustakas J (2009) ARA&A 47:159
28. Blanton MR, Schlegel DJ, Strauss MA et al (2005a) AJ 129:2562
29. Blanton MR, Lupton RH, Schlegel DJ et al (2005b) ApJ 631:208
30. Böhringer H, Briel UG, Schwarz RA et al (1994) Nature 368:828
31. Boissier S, Prantzos N (2000) MNRAS 312:398
32. Boissier S, Prantzos N, Boselli A, Gavazzi G (2003) MNRAS 346:1215
33. Boissier S, Boselli A, Duc P-A et al (2012) A&A 545:A142
34. Bolzonella M, Kovač K, Pozzetti L et al (2010) A&A 524:A76
35. Bonamente M, Lieu R, Nevalainen J, Kaastra JS (2001) ApJ 552:L7
36. Book LG, Benson AJ (2010) ApJ 716:810
37. Boselli A (2011) A panchromatic view of galaxies. In: Practical approach book, vol XVI. Wiley, New York 2011. ISBN-10: 3-527-40991-2. ISBN-13: 978-3-527-40991-4
38. Boselli A, Gavazzi G (2002) A&A 386:124
39. Boselli A, Gavazzi G (2006) PASP 118:517
40. Boselli A, Gavazzi G, Donas J, Scodeggio M (2001) AJ 121:753
41. Boselli A, Iglesias-Páramo J, Vílchez JM, Gavazzi G (2002) A&A 386:134
42. Boselli A, Cortese L, Deharveng JM et al (2005a) ApJ 629:L29
43. Boselli A, Boissier S, Cortese L et al (2005b) ApJ 623:L13
44. Boselli A, Boissier S, Cortese L et al (2006) ApJ 651:811
45. Boselli A, Boissier S, Cortese L, Gavazzi G (2008a) ApJ 674:742
46. Boselli A, Boissier S, Cortese L, Gavazzi G (2008b) A&A 489:1015
47. Boselli A, Boissier S, Cortese L et al (2009) ApJ 706:1527
48. Boselli A, Eales S, Cortese L et al (2010) PASP 122:261
49. Boselli A, Boissier S, Heinis S et al (2011) A&A 528:A107
50. Boselli A, Voyer E, Boissier S et al (2014a) A&A 570:A69
51. Boselli A, Cortese L, Boquien M et al (2014b) A&A 564:A67
52. Braglia FG, Pierini D, Biviano A, Boheringer H (2009) A&A 500:947
53. Briel UG, Henry JP, Boehringer H (1992) A&A 259:L31
54. Briel UG, Henry JP, Lumb DH et al (2001) A&A 365:L60
55. Brüggen M, De Lucia G (2008) MNRAS 383:1336
56. Cappellari M (2013) ApJ 778:L2
57. Cappellari M, Emsellem E, Krajnović D et al (2011a) MNRAS 413:813
58. Cappellari M, Emsellem E, Krajnović D et al (2011b) MNRAS 416:1680
59. Carter D, Goudfrooij P, Mobasher B et al (2008) ApJS 176:424
60. Cassata P, Guzzo L, Franceschini A et al (2007) ApJS 172:270
61. Catinella B, Schiminovich D, Cortese L et al (2013) MNRAS 436:34
62. Cayatte V, van Gorkom JH, Balkowski C, Kotanyi C (1990) AJ 100:604

63. Cen R, Pop A, Bachall N (2014) Proc Natl Acad Sci USA. (arXiv:1405.0537)
64. Chilingarian IV (2009) MNRAS 394:1229
65. Chung A, van Gorkom JH, Kenney JDP, Vollmer B (2007) ApJ 659:L115
66. Chung A, van Gorkom JH, Kenney JDP, Crowl H, Vollmer B (2009) AJ 138:1741
67. Churazov E, Vikhlinin A, Zhuravleva I et al (2012) MNRAS 421:1123
68. Cibinel A, Carollo CM, Lilly SJ et al (2013) ApJ 777:116
69. Cortese L, Hughes TM (2009) MNRAS 400:1225
70. Cortese L, Boselli A, Gavazzi G et al (2005) ApJ 623:L17
71. Cortese L, Boselli A, Buat V et al (2006a) ApJ 637:242
72. Cortese L, Gavazzi G, Boselli A et al (2006b) A&A 453:847
73. Cortese L, Marcillac D, Richard J et al (2007) MNRAS 376:157
74. Cortese L, Boselli A, Franzetti P et al (2008a) MNRAS 386:1157
75. Cortese L, Gavazzi G, Boselli A (2008b) MNRAS 390:1282
76. Cortese L, Minchin RF, Auld RR et al (2008c) MNRAS 383:1519
77. Cortese L, Davies JI, Pohlen M et al (2010) A&A 518:L49
78. Cortese L, Ciesla L, Boselli A et al (2012a) A&A 540:A52
79. Cortese L, Boissier S, Boselli A et al (2012b) A&A 544:A101
80. Côté P, Blakeslee JP, Ferrarese L et al (2004) ApJS 153:223
81. Côté P, Piatek S, Ferrarese L et al (2006) ApJS 165:57
82. Côté P, Ferrarese L, Jordán A et al (2007) ApJ 671:1456
83. Crawford SM, Bershady MA, Hoessel JG (2009) ApJ 690:1158
84. Davies J, Minchin R, Sabatini S et al (2004) MNRAS 349:922
85. Davies JI, Baes M, Bendo GJ et al (2010) A&A 518:L48
86. Davies JI, Bianchi S, Cortese L et al (2012) MNRAS 419:3505
87. Davies JI, Bianchi S, Baes M et al (2013) MNRAS 428:834
88. de Filippis E, Paolillo M, Longo G et al (2011) MNRAS 414:2771
89. de Looze I, Baes M, Zibetti S et al (2010) A&A 518:L54
90. de Looze I, Baes M, Boselli A, et al. (2013) MNRAS, 2280
91. De Lucia G (2011) Environment and the formation of galaxies: 30 years later. pp 203–210
92. De Lucia G, Poggianti BM, Aragón-Salamanca A et al (2004) ApJ 610:L77
93. De Lucia G, Poggianti BM, Aragón-Salamanca A et al (2007) MNRAS 374:809
94. De Lucia G, Poggianti BM, Halliday C et al (2009) MNRAS 400:68
95. De Lucia G, Weinmann S, Poggianti BM, Aragón-Salamanca A, Zaritsky D (2012) MNRAS 423:1277
96. den Brok M, Peletier RF, Valentijn EA et al (2011) MNRAS 414:3052
97. De Propris R, Phillipps S, Bremer MN (2013) MNRAS 434:3469
98. di Serego Alighieri S, Gavazzi G, Giovanardi C et al (2007) A&A 474:851
99. Dressler A (2004) Clusters of galaxies: probes of cosmological structure and galaxy. Evolution 206
100. Dressler A, Oemler A Jr, Poggianti BM et al (2013) ApJ 770:62
101. Drinkwater MJ, Gregg MD, Couch WJ et al (2004) PASA 21:375
102. Duc P-A, Bournaud F (2008) ApJ 673:787
103. Eales S, Dunne L, Clements D et al (2010) PASP 122:499
104. Eckert D, Neronov A, Courvoisier TJ-L, Produit N (2007) A&A 470:835
105. Ehlert S, Werner N, Simionescu A et al (2013) MNRAS 430:2401
106. Fabello S, Kauffmann G, Catinella B et al (2012) MNRAS 427:2841
107. Ferrarese L, Côté P, Jordán A et al (2006) ApJS 164:334
108. Ferrarese L, Côté P, Cuillandre J-C et al (2012) ApJS 200:4
109. Finoguenov A, Briel UG, Henry JP et al (2004a) A&A 419:47
110. Finoguenov A, Henriksen MJ, Briel UG, de Plaa J, Kaastra JS (2004b) ApJ 611:811
111. Font AS, Bower RG, McCarthy IG et al (2008) MNRAS 389:1619
112. Fontanot F, De Lucia G, Monaco P, Somerville RS, Santini P (2009) MNRAS 397:1776
113. Fossati M, Gavazzi G, Boselli A, Fumagalli M (2012) A&A 544:A128
114. Fossati M, Gavazzi G, Savorgnan G et al (2013) A&A 553:A91
115. Freeland E, Sengupta C, Croston J-H (2010) MNRAS 409:1518
116. Fritz J, Poggianti BM, Cava A et al (2014) A&A 566:A32
117. Fumagalli M, Krumholz MR, Prochaska JX, Gavazzi G, Boselli A (2009) ApJ 697:1811
118. Fumagalli M, Gavazzi G, Scaramella R, Franzetti P (2011) A&A 528:A46
119. Fumagalli M, Fossati M, Hau JKT, Gavazzi G, Bower R, Sun M, Boselli A (2014) (arXiv:1407.7527)
120. Gavazzi G, Jaffe W (1985) ApJ 294:L89
121. Gavazzi G, Jaffe W (1986) ApJ 310:53
122. Gavazzi G, Contursi A, Carrasco L et al (1995) A&A 304:325
123. Gavazzi G, Pierini D, Boselli A (1996) A&A 312:397

124. Gavazzi G, Catinella B, Carrasco L, Boselli A, Contursi A (1998) AJ 115:1745
125. Gavazzi G, Boselli A, Scodeggio M, Pierini D, Belsole E (1999) MNRAS 304:595
126. Gavazzi G, Boselli A, Mayer L et al (2001) ApJ 563:L23
127. Gavazzi G, Boselli A, Pedotti P, Gallazzi A, Carrasco L (2002) A&A 386:114
128. Gavazzi G, Boselli A, Donati A, Franzetti P, Scodeggio M (2003a) A&A 400:451
129. Gavazzi G, Cortese L, Boselli A et al (2003b) ApJ 597:210
130. Gavazzi G, Boselli A, van Driel W, O'Neil K (2005) A&A 429:439
131. Gavazzi G, Boselli A, Cortese L et al (2006a) A&A 446:839
132. Gavazzi G, O'Neil K, Boselli A, van Driel W (2006b) A&A 449:929
133. Gavazzi G, Giovanelli R, Haynes MP et al (2008) A&A 482:43
134. Gavazzi G, Fumagalli M, Cucciati O, Boselli A (2010) A&A 517:A73
135. Gavazzi G, Fumagalli M, Galardo V et al (2012) A&A 545:A16
136. Gavazzi G, Fumagalli M, Fossati M et al (2013a) A&A 553:A89
137. Gavazzi G, Savorgnan G, Fossati M et al (2013b) A&A 553:A90
138. Geha M, Guhathakurta P, van der Marel RP (2002) AJ 124:3073
139. Geha M, Guhathakurta P, van der Marel RP (2003) AJ 126:1794
140. Geha M, Blanton MR, Yan R, Tinker JL (2012) ApJ 757:85
141. Gil de Paz A, Boissier S, Madore BF et al (2007) ApJS 173:185
142. Gilbank DG, Balogh ML (2008) MNRAS 385:L116
143. Gilbank DG, Yee HKC, Ellingson E et al (2008) ApJ 673:742
144. Giodini S, Finoguenov A, Pierini D et al (2012) A&A 538:A104
145. Giovanelli R, Haynes MP, Kent BR et al (2005) AJ 130:2598
146. Giovanelli R, Haynes MP, Kent BR et al (2007) AJ 133:2569
147. Gnedin OY (2003) ApJ 582:141
148. Gómez PL, Nichol RC, Miller CJ et al (2003) ApJ 584:210
149. Graham AW, Guzmán R (2003) AJ 125:2936
150. Graham AW, Jerjen H, Guzmán R (2003) AJ 126:1787
151. Gunn JE, Gott JR III (1972) ApJ 176:1
152. Guo Q, White S, Boylan-Kolchin M et al (2011) MNRAS 413:101
153. Guo Q, Cole S, Eke V, Frenk C, Helly J (2013) MNRAS 434:1838
154. Haines CP, La Barbera F, Mercurio A, Merluzzi P, Busarello G (2006a) ApJ 647:L21
155. Haines CP, Merluzzi P, Mercurio A et al (2006b) MNRAS 371:55
156. Haines CP, Gargiulo A, La Barbera F et al (2007) MNRAS 381:7
157. Haines CP, Gargiulo A, Merluzzi P (2008) MNRAS 385:1201
158. Haines CP, Busarello G, Merluzzi P et al (2011) MNRAS 412:127
159. Hammer D, Hornschemeier AE, Mobasher B et al (2010a) ApJS 190:43
160. Hammer D, Verdoes Kleijn G, Hoyos C et al (2010b) ApJS 191:143
161. Hammer DM, Hornschemeier AE, Salim S et al (2012) ApJ 745:177
162. Hansen SM, Sheldon ES, Wechsler RH, Koester BP (2009) ApJ 699:1333
163. Hao C-N, Kennicutt RC, Johnson BD et al (2011) ApJ 741:124
164. Harsono D, de Propris R (2007) MNRAS 380:1036
165. Haynes M-P, Giovanelli R (1984) AJ 89:758
166. Haynes MP, Giovanelli R, Kent BR (2007) ApJ 665:L19
167. Haynes MP, Giovanelli R, Martin AM et al (2011) AJ 142:170
168. Henriques BMB, White SDM, Thomas PA et al (2013) MNRAS 431:3373
169. Hester JA (2006) ApJ 647:910
170. Hester JA, Seibert M, Neill JD et al (2010) ApJ 716:L14
171. Hickinbottom S, Simpson C, James P et al (2014) MNRAS 442:1286
172. Hogg DW, Blanton MR, Brinchmann J et al (2004) ApJ 601:L29
173. Huang S, Haynes MP, Giovanelli R, Brinchmann J (2012) ApJ 756:113
174. Hughes TM, Cortese L (2009) MNRAS 396:L41
175. Jáchym P, Kenney JDP, Ržuička A et al (2013) A&A 556:A99
176. Jáchym P, Combes F, Cortese L, Kenney JDP (2014) ApJ 792:11
177. Jaffe W, Gavazzi G (1986) AJ 91:204
178. Jaffé YL, Aragón-Salamanca A, De Lucia G et al (2011) MNRAS 410:280
179. Janz J, Lisker T (2008) ApJ 689:L25
180. Janz J, Lisker T (2009) ApJ 696:L102
181. Janz J, Laurikainen E, Lisker T et al (2012) ApJ 745:L24
182. Janz J, Laurikainen E, Lisker T et al (2014) ApJ 786:105
183. Jeltema TE, Binder B, Mulchaey JS (2008) ApJ 679:1162
184. Jerjen H, Kalnajs A, Binggeli B (2000) A&A 358:845

185. Jordán A, Blakeslee JP, Côté P et al (2007a) ApJS 169:213
186. Jordán A, McLaughlin DE, Côté P et al (2007b) ApJS 171:101
187. Kang X, van den Bosch FC (2008) ApJ 676:L101
188. Kantharia NG, Ananthakrishnan S, Nityananda R, Hota A (2005) A&A 435:483
189. Kapferer W, Kronberger T, Ferrari C, Riser T, Schindler S (2008) MNRAS 389:1405
190. Kapferer W, Sluka C, Schindler S, Ferrari C, Ziegler B (2009) A&A 499:87
191. Kauffmann G, White SDM, Heckman TM et al (2004) MNRAS 353:713
192. Kawata D, Mulchaey JS (2008) ApJ 672:L103
193. Kenney JDP, Tal T, Crowl HH, Feldmeier J, Jacoby GH (2008) ApJ 687:L69
194. Kenney JDP, Geha M, Jáchym P et al (2014) ApJ 780:119
195. Kilborn VA, Forbes DA, Barnes DG et al (2009) MNRAS 400:1962
196. Kennicutt RC Jr (1998) ARA&A 36:189
197. Kent BR (2010) ApJ 725:2333
198. Kent BR, Giovanelli R, Haynes MP et al (2007) ApJ 665:L15
199. Kent BR, Giovanelli R, Haynes MP et al (2008) AJ 136:713
200. Kent BR, Spekkens K, Giovanelli R et al (2009) ApJ 691:1595
201. Kim S, Rey S-C, Lisker T, Sohn ST (2010) ApJ 721:L72
202. Kimm T, Somerville RS, Yi SK et al (2009) MNRAS 394:1131
203. Kodama T, Balogh ML, Smail I, Bower RG, Nakata F (2004) MNRAS 354:1103
204. Koleva M, de Rijcke S, Prugniel P, Zeilinger WW, Michielsen D (2009) MNRAS 396:2133
205. Koleva M, Prugniel P, de Rijcke S, Zeilinger WW (2011) MNRAS 417:1643
206. Koleva M, Bouchard A, Prugniel P, De Rijcke S, Vauglin I (2013) MNRAS 428:2949
207. Koopmann RA, Kenney JDP, Young J (2001) ApJS 135:125
208. Koopmann RA, Haynes MP, Catinella B (2006) AJ 131:716
209. Kormendy J, Bender R (2012) ApJS 198:2
210. Kormendy J, Fisher DB, Cornell ME, Bender R (2009) ApJS 182:216
211. Kronberger T, Kapferer W, Unterguggenberger S, Schindler S, Ziegler BL (2008a) A&A 483:783
212. Kronberger T, Kapferer W, Ferrari C, Unterguggenberger S, Schindler S (2008b) A&A 481:337
213. Lanzoni B, Guiderdoni B, Mamon GA, Devriendt J, Hatton S (2005) MNRAS 361:369
214. Larson RB, Tinsley BM, Caldwell CN (1980) ApJ 237:692
215. Lemaux BC, Gal RR, Lubin LM et al (2012) ApJ 745:106
216. Lewis I, Balogh M, De Propris R et al (2002) MNRAS 334:673
217. Lieder S, Lisker T, Hilker M, Misgeld I, Durrell P (2012) A&A 538:A69
218. Lisker T (2009) Astron Nachr 330:1043
219. Lisker T, Han Z (2008) ApJ 680:1042
220. Lisker T, Fuchs B (2009) A&A 501:429
221. Lisker T, Grebel EK, Binggeli B (2006a) AJ 132:497
222. Lisker T, Glatt K, Westera P, Grebel EK (2006b) AJ 132:2432
223. Lisker T, Grebel EK, Binggeli B, Glatt K (2007) ApJ 660:1186
224. Lisker T, Grebel EK, Binggeli B (2008) AJ 135:380
225. Lisker T, Janz J, Hensler G et al (2009) ApJ 706:L124
226. Lisker T, Weinmann SM, Janz J, Meyer HT (2013) MNRAS 432:1162
227. Marinova I, Jogee S, Weinzirl T et al (2012) ApJ 746:136
228. Martin DC, Fanson J, Schiminovich D et al (2005) ApJ 619:L1
229. Martin DC, Wyder TK, Schiminovich D et al (2007) ApJS 173:342
230. Martin AM, Papastergis E, Giovanelli R et al (2010) ApJ 723:1359
231. Mastropietro C, Moore B, Mayer L et al (2005) MNRAS 364:607
232. Mayer L, Governato F, Colpi M et al (2001a) ApJ 559:754
233. Mayer L, Governato F, Colpi M et al (2001b) ApJ 547:L123
234. Mayer L, Mastropietro C, Wadsley J, Stadel J, Moore B (2006) MNRAS 369:1021
235. McCarthy IG, Frenk CS, Font AS et al (2008) MNRAS 383:593
236. McConnachie AW, Venn KA, Irwin MJ, Young LM, Geehan JJ (2007) ApJ 671:L33
237. McDonald M, Courteau S, Tully RB, Roediger J (2011) MNRAS 414:2055
238. McGee SL, Balogh ML, Bower RG, Font AS, McCarthy IG (2009) MNRAS 400:937
239. Mei S, Blakeslee JP, Côté P et al (2007) ApJ 655:144
240. Mercurio A, Merluzzi P, Haines CP et al (2006) MNRAS 368:109
241. Merluzzi P, Mercurio A, Haines CP et al (2010) MNRAS 402:753
242. Merluzzi P, Busarello G, Dopita MA et al (2013) MNRAS 429:1747
243. Michielsen D, Boselli A, Conselice CJ et al (2008) MNRAS 385:1374
244. Misgeld I, Hilker M (2011) MNRAS 414:3699
245. Misgeld I, Mieske S, Hilker M (2008) A&A 486:697

246. Misgeld I, Hilker M, Mieske S (2009) A&A 496:683
247. Mok A, Balogh ML, McGee SL et al (2013) MNRAS 431:1090
248. Moore B, Katz N, Lake G, Dressler A, Oemler A (1996) Nature 379:613
249. Mulchaey JS (2000) ARA&A 38:289
250. Mulchaey JS, Zabludoff AI (1998) ApJ 496:73
251. Mulchaey JS, Davis DS, Mushotzky RF, Burstein D (2003) ApJS 145:39
252. Murakami H, Baba H, Barthel P et al (2007) PASJ 59:369
253. Murakami H, Komiyama M, Matsushita K et al (2011) PASJ 63:963
254. Neumann DM, Arnaud M, Gastaud R et al (2001) A&A 365:L74
255. O'Connell RW (1999) ARA&A 37:603
256. Okamoto T, Nagashima M (2003) ApJ 587:500
257. Oosterloo T, van Gorkom J (2005) A&A 437:L19
258. Osmond JPF, Ponman TJ (2004) MNRAS 350:1511
259. Paudel S, Lisker T, Kuntschner H, Grebel EK, Glatt K (2010a) MNRAS 405:800
260. Paudel S, Lisker T, Janz J (2010b) ApJ 724:L64
261. Paudel S, Lisker T, Kuntschner H (2011) MNRAS 413:1764
262. Paudel S, Duc P-A, Côté P et al (2013) ApJ 767:133
263. Pedraz S, Gorgas J, Cardiel N, Sánchez-Blázquez P, Guzmán R (2002) MNRAS 332:L59
264. Peng EW, Jordán A, Côté P et al (2008) ApJ 681:197
265. Penny SJ, Conselice CJ, de Rijcke S et al (2011) MNRAS 410:1076
266. Poggianti BM, Bridges TJ, Komiyama Y et al (2004) ApJ 601:197
267. Poggianti BM, Aragón-Salamanca A, Zaritsky D et al (2009) ApJ 693:112
268. Poggianti B-M, De Lucia G, Varela J et al (2010) MNRAS 405:995
269. Poggianti BM, Calvi R, Bindoni D et al (2013) ApJ 762:77
270. Popesso P, Böhringer H, Romaniello M, Voges W (2005) A&A 433:415
271. Popesso P, Biviano A, Böhringer H, Romaniello M (2006) A&A 445:29
272. Popesso P, Biviano A, Romaniello M, Böhringer H (2007) A&A 461:411
273. Rasmussen J, Ponman TJ, Verdes-Montenegro L, Yun MS, Borthakur S (2008) MNRAS 388:1245
274. Rasmussen J, Mulchaey JS, Bai L et al (2012a) ApJ 757:122
275. Rasmussen J, Bai X-N, Mulchaey JS et al (2012b) ApJ 747:31
276. Renaud M, Bélanger G, Paul J, Lebrun F, Terrier R (2006) A&A 453:L5
277. Rines K, Geller MJ (2008) AJ 135:1837
278. Rines K, Geller MJ, Kurtz MJ, Diaferio A (2005) AJ 130:1482
279. Robotham A, Phillipps S, de Propris R (2010) MNRAS 403:1812
280. Roediger E (2009) Astron Nachr 330:888
281. Roediger E, Hensler G (2005) A&A 433:875
282. Roediger E, Brüggen M (2006) MNRAS 369:567
283. Roediger E, Brüggen M (2007) MNRAS 380:1399
284. Rudnick G, von der Linden A, Pelló R et al (2009) ApJ 700:1559
285. Rudnick GH, Tran K-V, Papovich C, Momcheva I, Willmer C (2012) ApJ 755:14
286. Ruszkowski M, Brüggen M, Lee D, Shin M-S (2014) ApJ 784:75
287. Ryś A, Falcón-Barroso J, van de Ven G (2013) MNRAS 428:2980
288. Sakai S, Kennicutt RC Jr, van der Hulst JM, Moss C (2002) ApJ 578:842
289. Sánchez SF, Kennicutt RC, Gil de Paz A et al (2012) A&A 538:A8
290. Sánchez-Janssen R, Aguerri JAL (2012) MNRAS 424:2614
291. Sandage A, Binggeli B, Tammann GA (1985) AJ 90:1759
292. Sarazin CL (1986) Rev Mod Phys 58:1
293. Schawinski K, Virani S, Simmons B et al (2009) ApJ 692:L19
294. Schawinski K, Urry CM, Simmons BD et al (2014) MNRAS 440:889
295. Scott TC, Cortese L, Brinks E et al (2012) MNRAS 419:L19
296. Scott TC, Usero A, Brinks E et al (2013) MNRAS 429:221
297. Sengupta C, Balasubramanyam R, Dwarakanath KS (2007) MNRAS 378:137
298. Shibata R, Matsushita K, Yamasaki NY et al (2001) ApJ 549:228
299. Smith RJ, Hudson MJ, Lucey JR, Nelan JE, Wegner GA (2006) MNRAS 369:1419
300. Smith RJ, Lucey JR, Hudson MJ (2007) MNRAS 381:1035
301. Smith RJ, Marzke RO, Hornschemeier AE et al (2008) MNRAS 386:L96
302. Smith RJ, Lucey JR, Hudson MJ et al (2009) MNRAS 392:1265
303. Smith RJ, Lucey JR, Hammer D et al (2010) MNRAS 408:1417
304. Smith RJ, Lucey JR, Price J, Hudson MJ, Phillipps S (2012a) MNRAS 419:3167
305. Smith RJ, Lucey JR, Carter D (2012b) MNRAS 421:2982
306. Smith R, Fellhauer M, Assmann P (2012c) MNRAS 420:1990

307. Smith R, Duc PA, Candlish GN et al (2013) MNRAS 2255
308. Smith Castelli AV, Bassino LP, Richtler T et al (2008) MNRAS 386:2311
309. Smith Castelli AV, González NM, Faifer FR, Forte JC (2013) ApJ 772:68
310. Solanes JM, Manrique A, García-Gómez C et al (2001) ApJ 548:97
311. Springel V, White SDM, Jenkins A et al (2005) Nature 435:629
312. Stott JP, Smail I, Edge AC et al (2007) ApJ 661:95
313. Stott JP, Pimbblet KA, Edge AC, Smith GP, Wardlow JL (2009) MNRAS 394:2098
314. Strauss MA, Weinberg DH, Lupton RH et al (2002) AJ 124:1810
315. Sun M, Donahue M, Voit GM (2007) ApJ 671:190
316. Sun M, Voit GM, Donahue M et al (2009) ApJ 693:1142
317. Sun M, Donahue M, Roediger E et al (2010) ApJ 708:946
318. Taranu DS, Hudson MJ, Balogh ML et al (2014) MNRAS 440:1934
319. Taylor R, Davies JI, Auld R, Minchin RF (2012) MNRAS 423:787
320. Taylor R, Davies JI, Auld R, Minchin RF, Smith R (2013) MNRAS 428:459
321. Thomas D, Maraston C, Schawinski K, Sarzi M, Silk J (2010) MNRAS 404:1775
322. Toloba E, Boselli A, Gorgas J et al (2009) ApJ 707:L17
323. Toloba E, Boselli A, Cenarro AJ et al (2011) A&A 526:A114
324. Toloba E, Boselli A, Peletier RF et al (2012) A&A 548:A78
325. Toloba E, Guhathakurta P, Peletier R et al (2014a) ApJS (in press)
326. Toloba E, Guhathakurta P, Boselli A et al (2014b) ApJ (in press)
327. Toloba E, Guhathakurta P, van de Ven G et al (2014c) ApJ 783:120
328. Tonnesen S, Bryan G-L (2012) MNRAS 422:1609
329. Tonnesen S, Bryan GL, van Gorkom JH (2007) ApJ 671:1434
330. Tonnesen S, Bryan GL (2009) ApJ 694:789
331. Urban O, Werner N, Simionescu A, Allen SW, Böhringer H (2011) MNRAS 414:2101
332. van den Bosch FC, Aquino D, Yang X et al (2008) MNRAS 387:79
333. van Zee L, Skillman ED, Haynes MP (2004) AJ 128:121
334. Verdes-Montenegro L, Yun MS, Borthakur S, Rasmussen J, Ponman T (2007) New Astron Rev 51:87
335. Verdugo M, Ziegler BL, Gerken B (2008) A&A 486:9
336. Vikhlinin A, Markevitch M, Forman W, Jones C (2001) ApJ 555:L87
337. Vijayaraghavan R, Ricker PM (2013) MNRAS 435:2713
338. Vollmer B, Cayatte V, Balkowski C, Duschl WJ (2001) ApJ 561:708
339. Voyer E, Boselli A, Boissier S et al (2014) A&a (in press)
340. Vulcani B, Poggianti BM, Oemler A et al (2013) A&A 550:A58
341. Wang L, Weinmann SM, Neistein E (2012) MNRAS 421:3450
342. Wetzel AR, Tinker JL, Conroy C, van den Bosch FC (2013) MNRAS 432:336
343. Weinmann SM, Lisker T, Guo Q, Meyer HT, Janz J (2011) MNRAS 416:1197
344. Weżgowiec M, Bomans DJ, Ehle M et al (2012) A&A 544:A99
345. Wilman DJ, Zibetti S, Budavári T (2010) MNRAS 406:1701
346. Wright EL, Eisenhardt PRM, Mainzer AK et al (2010) AJ 140:1868
347. Wyder TK, Treyer MA, Milliard B et al (2005) ApJ 619:L15
348. Yagi M, Komiyama Y, Yoshida M et al (2007) ApJ 660:1209
349. Yagi M, Yoshida M, Komiyama Y et al (2010) AJ 140:1814
350. Yagi M, Gu L, Fujita Y et al (2013) ApJ 778:91
351. Yamagami T, Fujita Y (2011) PASJ 63:1165
352. York DG, Adelman J, Anderson JE Jr et al (2000) AJ 120:1579
353. Yoshida M, Ohyama Y, Iye M et al (2004) AJ 127:90
354. Yoshida M, Yagi M, Komiyama Y et al (2008) ApJ 688:918
355. Yoshida M, Yagi M, Komiyama Y et al (2012) ApJ 749:43
356. Zandivarez A, Martínez HJ (2011) MNRAS 415:2553
357. Zandivarez A, Martínez HJ, Merchán ME (2006) ApJ 650:137
358. Zhang B, Sun M, Ji L et al (2013) ApJ 777:122